

# Bayesian probabilistic propagation of hybrid uncertainties: Estimation of response **expectation** function, its variable importance and bounds

Chao Dang<sup>a</sup>, Pengfei Wei<sup>b,\*</sup>, Matthias G.R. Faes<sup>c</sup>, Michael Beer<sup>a,d,e</sup>

<sup>a</sup>*Institute for Risk and Reliability, Leibniz University Hannover, Callinstr. 34, Hannover 30167, Germany*

<sup>b</sup>*School of Power and Energy, Northwestern Polytechnical University, Xi'an 710072, PR China*

<sup>c</sup>*Chair for Reliability Engineering, TU Dortmund University, Leonhard-Euler-Str. 5, Dortmund 44227, Germany*

<sup>d</sup>*Institute for Risk and Uncertainty, University of Liverpool, Liverpool L69 7ZF, United Kingdom*

<sup>e</sup>*International Joint Research Center for Resilient Infrastructure & International Joint Research Center for Engineering Reliability and Stochastic Mechanics, Tongji University, Shanghai 200092, PR China*

---

## Abstract

Uncertainties existing in physical and engineering systems can be characterized by different kinds of mathematical models according to their respective features. However, efficient propagation of hybrid uncertainties via an expensive-to-evaluate computer simulator is still a computationally challenging task. In this contribution, estimation of response **expectation** function (**REF**), its variable importance and bounds under hybrid uncertainties in the form of precise probability models, parameterized probability-box models and interval models is investigated through a Bayesian approach. Specifically, a new method, termed “Parallel Bayesian Quadrature Optimization” (PBQO), is developed. The method starts by treating the **REF** estimation as a Bayesian probabilistic integration (BPI) problem with a Gaussian process (GP) prior, which in turn implies a GP posterior for the **REF**. Then, one acquisition function originally developed in BPI and other two in Bayesian global optimization are introduced for Bayesian experimental designs. Besides, an innovative strategy is also proposed to realize multi-point selection at each iteration. Overall, a novel advantage of PBQO is that it is capable of yielding the **REF**, its variable importance and bounds simultaneously via a pure single-loop procedure allowing for parallel computing. Three numerical examples are studied to demonstrate the performance of the proposed method over existing methods.

*Keywords:* Hybrid uncertainties, Response expectation function, Bayesian probabilistic integration, Bayesian global optimization, Bayesian experimental design, Parallel computing

---

## 1. Introduction

Uncertainty quantification (UQ) is a hot topic and even research frontier in a broad range of modern science and engineering fields. UQ is primarily aimed at the quantitative characterization and consequent

---

\*Corresponding author

*Email addresses:* [chao.dang@irz.uni-hannover.de](mailto:chao.dang@irz.uni-hannover.de) (Chao Dang), [pengfeiwei@nwpu.edu.cn](mailto:pengfeiwei@nwpu.edu.cn) (Pengfei Wei), [matthias.faes@tu-dortmund.de](mailto:matthias.faes@tu-dortmund.de) (Matthias G.R. Faes), [beer@irz.uni-hannover.de](mailto:beer@irz.uni-hannover.de) (Michael Beer)

30 reduction of uncertainties in both physical and engineering systems. Uncertainties occur when all or some  
31 aspects of the system under consideration are not exactly known. Examples of such aspects include, e.g., sys-  
32 tem parameters and operating conditions. These uncertainties generally originate from a variety of sources  
33 such as **inherent variation**, manufacturing error, modelling **assumptions** or a combination hereof. In terms  
34 of the origin of uncertainties, they are typically classified into either aleatory or epistemic types [1, 2].  
35 Aleatory uncertainty refers to the uncertainty due to the intrinsic randomness or variability, and thus is  
36 irreducible in nature. As such, aleatory uncertainty is an inherent property of the system under consider-  
37 ation. Epistemic uncertainty, on the other hand, is associated with a lack of knowledge (or information)  
38 on the side of the analysts, and hence can be potentially reduced or even eliminated by acquiring more  
39 knowledge. Commonly, these two types of uncertainties occur together in both science and engineering, and  
40 many different uncertainty models **might appear** simultaneously in **just one single problem**. In addition to  
41 characterizing these uncertainties with appropriate mathematical models, uncertainty propagation through  
42 a computational model has **also** been of central interest from both academia and industry.

43 Many approaches have been indeed developed to quantitatively describe uncertain phenomena, which  
44 can be broadly categorized into three major groups: probabilistic approach, non-probabilistic approach and  
45 imprecise probability approach. The probabilistic approach is rooted in classical probability theory, and is  
46 the most traditional way to quantify uncertainties. Following this approach, non-determinism is modelled  
47 by a precise probability distribution on the basis of a set of probability axioms [3]. Despite its rigor in theory  
48 and popularity in practical applications, it is often criticized that the probabilistic approach indispensably  
49 relies on very fine information, e.g., a large amount of high-quality data, which is not always available.  
50 Alternatively, the non-probabilistic approach, including interval models [4], fuzzy sets [5] and convex models  
51 [6], is emerging for characterizing uncertainty with limited information, where the variation bounds need  
52 to be specified, instead of a precise probability distribution. However, it is argued that these methods  
53 are mostly suitable to deal with epistemic uncertainty. In recent years, the imprecise probability approach  
54 has gained increasing attention as a promising framework to quantify complex uncertainties, particularly  
55 when the available information or data is not sufficient to identify a unique probability distribution [7]. In  
56 essence, it is an extension to classical probability theory where the uncertainty is characterised by a set of  
57 probability measures, rather than a single one. Therefore, it allows for modelling both aleatory uncertainty  
58 and epistemic uncertainty separately within a uniform framework. Typically, the aleatory uncertainty is  
59 characterized by the traditional probabilistic models, and the epistemic uncertainty is handled by the non-  
60 probabilistic models. Representative techniques include the probability box (p-box) [8], evidence theory [9]  
61 and fuzzy probability [10] among others.

62 As for uncertainty propagation, great efforts have been made along each line of uncertainty characteriza-  
63 tion over the past several decades. The existing approaches for propagating precise probabilistic uncertainty  
64 can be roughly divided into five categories: stochastic simulation methods [11–13], approximate analytical

65 methods [14, 15], surrogate-assisted methods [16–18], numerical integration methods [19–23] and probability  
66 conservation-based methods [24, 25]. Differently, the propagation of non-probabilistic uncertainty follows  
67 another distinct philosophy, more relying on, e.g., interval arithmetic [26], optimization methods [27, 28],  
68 perturbation methods [29, 30] and etc. Also advanced sampling approaches for interval analysis have been  
69 introduced [31, 32]. One can refer to [5] for a good review on recent trends in propagation of non-probabilistic  
70 uncertainty. For imprecise probability propagation, however, the above two kinds of methods are not suit-  
71 able, and hence new developments are necessary. The most common way to address the problem involves a  
72 double-loop procedure that uses the aforementioned two types of methods in a nested way, such as optimized  
73 parameter sampling [33] and interval Monte Carlo simulation [34], which often suffers from a heavy com-  
74 putational burden. To improve the computational efficiency, decoupled strategies have recently attracted  
75 **increasing** attention, and representative works include the augmented subset simulation [35], non-intrusive  
76 imprecise stochastic simulation [36, 37], operator norm theory [38], active learning augmented probabilistic  
77 integration [39], non-intrusive imprecise probabilistic integration (NIPI) [40], and collaborative and adaptive  
78 Bayesian optimization (CABO) [41]. For an review of the computation methods for propagating p-boxes,  
79 the reader is referred to [42]. Besides, some progress has also been made in the context of hybrid uncertainty  
80 propagation, e.g., surrogate modelling-based methods [43–48], stochastic simulation-based methods [49–51]  
81 and others [52, 53]. For propagating probabilistic-interval hybrid uncertainty, one can refer to the review  
82 [54]. Overall, propagation of hybrid uncertainties poses a more significant computational challenge in UQ  
83 community, and the existing mythologies are far from desirable for general practical applications.

84 In this paper, a novel method is presented to propagate hybrid uncertainties in the form of precise  
85 probabilistic models, parameterized p-box models and interval models, where the response expectation  
86 function (REF), its variable importance and bounds are of concern. The method belongs to the class of  
87 Bayesian probabilistic numerical methods [55], and can also be seen as an important extension to the NIPI  
88 [40] and CABO [41] methods originally developed for propagating parameterized p-box models. **The main**  
89 **contributions of the present work can be summarized as follows:**

- 90 • A general Bayesian framework is presented for propagating hybrid uncertainties, which is non-intrusive  
91 and fully decoupled in nature;
- 92 • Posterior means and variances of the REF and its random-sampling high-dimensional model represen-  
93 tation (RS-HDMR) decomposition are analytically derived in closed form;
- 94 • Parallelized Bayesian experiment design is realized so as to take advantage of parallel computing at  
95 each iteration;
- 96 • A Matlab implementation of our methodology is freely available to the public <sup>1</sup>.

---

<sup>1</sup>to be released upon acceptance of the paper

97 The remaining of this paper is organized as follows. We start by stating the problem to be solved in this  
98 study in Section 2. Section 3 presents the theoretical basis and numerical implementation procedure of the  
99 proposed method, **with the relationship to the existing NIPI and CABO methods being discussed**. How to  
100 extend the proposed method to a relatively more general case of hybrid uncertainties is briefly explained in  
101 Section 4. In Section 5, three numerical examples are studied to demonstrate the proposed method. The  
102 paper ends with some concluding remarks and perspectives in Section 6.

## 103 2. Problem statement

104 In this work, three kinds of uncertainty characterization models are considered to model non-deterministic  
105 inputs of a computer **simulator**, i.e., precise probability models, parameterized p-box models and interval  
106 models. The precise probability models that are deeply rooted in probability theory are assumed to be used  
107 for describing pure aleatory uncertainty. As a representative of imprecise probabilities, the parameterized p-  
108 box models are able to account for both aleatory uncertainty and epistemic uncertainty simultaneously. The  
109 interval models serve as a representative of non-probabilistic models and are useful to model the constant-  
110 but-unknown epistemic uncertainty. As such, the developed method is expected to work in the following  
111 four cases:

- 112 **Case I:** Precise probabilistic models and parameterized p-box models coexist in the model inputs;
- 113 **Case II:** Only parameterized p-box models exist in the model inputs;
- 114 **Case III:** Precise probabilistic models and interval models coexist in the model inputs;
- 115 **Case IV:** Precise probabilistic models, parameterized p-box models and interval models coexist in the  
116 model inputs.

117 Among the four cases, **Case IV** constitutes a more general situation of hybrid uncertainties. For  
118 notational clarity, however, we only take **Case III** as an example to illustrate the proposed method in  
119 the following, and when it comes to the general case (i.e., **Case IV**) one can refer to Section 4. Let  
120  $\mathbf{X} = [X_1, X_2, \dots, X_{d_1}] \in \mathcal{X} \subseteq \mathbb{R}^{d_1}$  and  $\mathbf{A} = [A_1, A_2, \dots, A_{d_2}] \in \mathcal{A} \subseteq \mathbb{R}^{d_2}$  denote a  $d_1$ -dimensional vector  
121 of precise random variables and a  $d_2$ -dimensional vector of interval variables, respectively. The random  
122 variables are said to be ‘precise’ when their distribution types and distribution parameters are exactly  
123 known, and we assume that the joint probability density function (PDF) of  $\mathbf{X}$  exists, denoted as  $f_{\mathbf{X}}(\mathbf{x})$ .  
124 The interval variables refer to the uncertain parameters with limited information, and can only be specified  
125 by their lower and upper bounds, i.e.,  $\mathbf{A} = [\underline{\alpha}, \bar{\alpha}]$ , where  $\underline{\alpha} = [\alpha_1, \alpha_2, \dots, \alpha_{d_2}]$  and  $\bar{\alpha} = [\bar{\alpha}_1, \bar{\alpha}_2, \dots, \bar{\alpha}_{d_2}]$ . As  
126 such,  $\mathbf{A}$  represents a  $d_2$ -dimensional hyper-rectangle. In this study, these  $d_1 + d_2$  variables are assumed to be  
127 independent just for the convenience of describing our method. The computer simulator is represented by  
128 a deterministic, continuous and real-valued function  $g : \mathbb{R}^{d_1+d_2} \mapsto \mathbb{R}, \{x, \alpha\} \rightarrow z$ , with  $Z = g(\mathbf{X}, \mathbf{A})$  being  
129 a scalar quantity of interest. Due to the existence of interval variables,  $Z$  is no longer a random variable

130 unless  $\mathbf{A}$  is fixed at a value  $\boldsymbol{\alpha} \in \mathbf{A}$ . Thus, the expectation of  $Z$ , is not a deterministic values anymore, but  
 131 function of the interval variables. More precisely, it only assume a crisp value for a realisation of the input  
 132 intervals. To formalize, the definition of the so-called REF is given as follows:

$$m(\boldsymbol{\alpha}) = \int_{\mathcal{X}} g(\mathbf{x}, \boldsymbol{\alpha}) f_{\mathbf{X}}(\mathbf{x}) d\mathbf{x}, \quad (1)$$

133 The lower and upper bounds of  $m(\boldsymbol{\alpha})$  can be defined as:

$$m_l = \min_{\boldsymbol{\alpha} \in [\underline{\boldsymbol{\alpha}}, \bar{\boldsymbol{\alpha}}]} m(\boldsymbol{\alpha}) = \min_{\boldsymbol{\alpha} \in [\underline{\boldsymbol{\alpha}}, \bar{\boldsymbol{\alpha}}]} \int_{\mathcal{X}} g(\mathbf{x}, \boldsymbol{\alpha}) f_{\mathbf{X}}(\mathbf{x}) d\mathbf{x}, \quad (2)$$

$$m_u = \max_{\boldsymbol{\alpha} \in [\underline{\boldsymbol{\alpha}}, \bar{\boldsymbol{\alpha}}]} m(\boldsymbol{\alpha}) = \max_{\boldsymbol{\alpha} \in [\underline{\boldsymbol{\alpha}}, \bar{\boldsymbol{\alpha}}]} \int_{\mathcal{X}} g(\mathbf{x}, \boldsymbol{\alpha}) f_{\mathbf{X}}(\mathbf{x}) d\mathbf{x}. \quad (3)$$

135 The REF can provide complete information about how the response expectation changes with its argu-  
 136 ment  $\boldsymbol{\alpha}$ , whereas the interval  $[m_l, m_u]$  measures the amount of epistemic uncertainty present in the response  
 137 expectation. Besides, the analyst may also concern the variable importance of the REF. Intuitively, the  
 138 bounds and variable importance analysis of the REF can be proceeded straightforwardly once the REF  
 139 is available. However, it is still a non-trivial task to compute the REF in an efficient manner since each  
 140 evaluation of the response function  $g(\mathbf{x}, \boldsymbol{\alpha})$  can be prohibitively expensive for a real-world problem.

### 141 3. Parallel Bayesian quadrature optimization

142 As the REF defined in Eq. (1) is given in the form of an integral, the Bayesian probabilistic integration  
 143 (BPI) [23] can be applied to efficiently obtain an estimate for the REF. If we assign a Gaussian process (GP)  
 144 prior for the integrand  $g(\mathbf{x}, \boldsymbol{\alpha})$ , the induced posterior of the REF is also a GP. Following this, the lower and  
 145 upper bounds defined in Eqs. (2) and (3) may be further solved by the Bayesian global optimization (BGO)  
 146 [56]. In this section, a novel Bayesian approach combining the BPI and BGO, called Parallel Bayesian  
 147 Quadrature Optimization (PBQO), is presented to produce the REF, its variable importance and bounds  
 148 simultaneously in an efficient manner.

#### 149 3.1. Variable transformation

150 Before introducing our method, a pre-processing step should be performed to transform the original input  
 151 variable vector  $\{\mathbf{X}, \mathbf{A}\}$  to a new one so as to make the proposed method analytically tractable. In this study,  
 152 the random variable vector  $\mathbf{X}$  is transformed to be a standard normal one by a certain transformation (e.g.,  
 153 isoprobabilistic transformation), which is denoted as  $\mathbf{U} = T_1(\mathbf{X})$ . In contrast, we consider transforming  
 154 the **interval** vector  $\mathbf{A}$  to be a **standard** one (i.e.,  $[0, 1]^{d_2}$ ) by a simple linear transformation such that  $\mathbf{V} =$   
 155  $T_2(\mathbf{A})$ . For convenience, the two transformations can be written in a uniform form  $\mathbf{W} = T(\mathbf{X}, \mathbf{A})$ , where  
 156  $\mathbf{W} = \{\mathbf{U}, \mathbf{V}\}$ . The REF with respect to  $\mathbf{v}$  is defined as:

$$\mathcal{M}(\mathbf{v}) = \int_{\mathcal{U}} \mathcal{G}(\mathbf{w}) f_{\mathbf{U}}(\mathbf{u}) d\mathbf{u}, \quad (4)$$

157 where  $\mathcal{G}(\mathbf{w}) = g(T(\mathbf{x}, \boldsymbol{\alpha}))$ ,  $f_{\mathbf{U}}(\mathbf{u})$  is the joint PDF of  $\mathbf{U}$ . Once  $\mathcal{M}(\mathbf{v})$  is available,  $m(\boldsymbol{\alpha})$  can be easily  
 158 obtained as  $m(\boldsymbol{\alpha}) = \mathcal{M}(T_2(\boldsymbol{\alpha}))$ . Note that the  $T_1$  transformation is necessary for the analytical tractability  
 159 of the proposed method, while  $T_2$  transformation is not. However, we introduce the  $T_2$  transformation only  
 160 for the purpose of producing concise analytical expressions.

### 161 3.2. Prior Gaussian process

162 In the proposed PBQO method, we first place a GP prior over the space  $\mathcal{G}$  of functions:  $\mathcal{G} : \mathcal{W} \rightarrow \mathbb{R}$ ,  
 163 denoted as  $\hat{\mathcal{G}}(\mathbf{w}) \sim \mathcal{GP}(\mu_0(\mathbf{w}), k_0(\mathbf{w}, \mathbf{w}'))$ , where  $\mu_0(\mathbf{w})$  and  $k_0(\mathbf{w}, \mathbf{w}')$  are the prior mean and covariance  
 164 functions, respectively. The prior mean function reflects the general trend of the GP, and can be assumed to  
 165 be, e.g., zero, constant or a linear polynomial. The covariance function is a more crucial ingredient of the GP  
 166 since it encodes our basic assumptions about the function to be inferred, e.g., smoothness and periodicity.  
 167 In this study, the prior mean function adopts a constant, i.e.,  $\mu_0(\mathbf{w}) = \beta$ , and the prior covariance function  
 168 takes the squared exponential kernel:

$$\begin{aligned} k_0(\mathbf{w}, \mathbf{w}') &= s_0^2 \exp \left[ -\frac{1}{2} (\mathbf{w} - \mathbf{w}')^\top \boldsymbol{\Sigma}^{-1} (\mathbf{w} - \mathbf{w}') \right] \\ &= s_0^2 \exp \left[ -\frac{1}{2} (\mathbf{u} - \mathbf{u}')^\top \boldsymbol{\Sigma}_{\mathbf{u}}^{-1} (\mathbf{u} - \mathbf{u}') \right] \exp \left[ -\frac{1}{2} (\mathbf{v} - \mathbf{v}')^\top \boldsymbol{\Sigma}_{\mathbf{v}}^{-1} (\mathbf{v} - \mathbf{v}') \right], \end{aligned} \quad (5)$$

169 where  $s_0^2$  is the process variance,  $\boldsymbol{\Sigma} = \text{diag} \{l_1^2, l_2^2, \dots, l_{d_1+d_2}^2\}$  with  $l_i$  being the characteristic lengthscale in  
 170  $i$ -th dimension,  $\boldsymbol{\Sigma}_{\mathbf{u}} = \text{diag} \{l_1^2, l_2^2, \dots, l_{d_1}^2\}$  and  $\boldsymbol{\Sigma}_{\mathbf{v}} = \text{diag} \{l_{d_1+1}^2, l_{d_1+2}^2, \dots, l_{d_1+d_2}^2\}$ ; Throughout the paper,  
 171 the symbol  $\text{diag} \{\cdot\}$  means to create a square diagonal matrix with the elements of its argument when its  
 172 argument is a vector or to get a column vector of the diagonal elements of its argument when its argument  
 173 is a matrix. The parameters  $\beta, s_0, l_1, l_2, \dots, l_{d_1+d_2}$  are called hyperparameters. Note that the analytical  
 174 tractability of the proposed method relies on using the squared exponential kernel.

### 175 3.3. Bayesian posterior inference

176 Suppose that we have evaluated the  $\mathcal{G}$ -function at  $n$  points. Let a  $n \times (d_1 + d_2)$  matrix  $\mathcal{W} = (\mathbf{U}, \mathbf{V}) =$   
 177  $\{\mathbf{w}^{(j)}\}_{j=1}^n$  denote the  $n$  points at which the  $\mathcal{G}$ -function are evaluated, and a  $n \times 1$  matrix  $\mathcal{Z} = \{z^{(j)}\}_{j=1}^n$   
 178 denote the corresponding  $\mathcal{G}$ -function values at  $\mathcal{W}$ . Given  $\mathcal{D} = \{\mathcal{W}, \mathcal{Z}\}$ , the hyperparameters involved in  
 179 the prior mean and covariance functions can be determined by, e.g., maximum likelihood estimation [57].  
 180 Besides, conditioning on the data  $\mathcal{D}$ , we can arrive at a posterior GP over functions  $\mathcal{G} \in \mathcal{G}$ , which is denoted  
 181 as  $\mathcal{GP}(\mu_n(\mathbf{w}), k_n(\mathbf{w}, \mathbf{w}'))$ . According to [57], the posterior mean  $\mu_n(\mathbf{w})$  and posterior covariance function  
 182  $k_n(\mathbf{w}, \mathbf{w}')$  can be given by:

$$\mu_n(\mathbf{w}) = \mu_0(\mathbf{w}) + \mathbf{k}_0(\mathbf{w}, \mathcal{W})^\top \mathbf{K}_0^{-1} (\mathcal{Z} - \mu_0(\mathcal{W})), \quad (6)$$

$$k_n(\mathbf{w}, \mathbf{w}') = k_0(\mathbf{w}, \mathbf{w}') - \mathbf{k}_0(\mathbf{w}, \mathcal{W})^\top \mathbf{K}_0^{-1} \mathbf{k}_0(\mathbf{w}', \mathcal{W}), \quad (7)$$

184 where  $\boldsymbol{\mu}_0(\mathcal{W}) = [\mu_0(\mathbf{w}^{(1)}), \mu_0(\mathbf{w}^{(2)}), \dots, \mu_0(\mathbf{w}^{(n)})]^\top$  is the mean vector at  $\mathcal{W}$ ;  $\mathbf{k}_0(\mathbf{w}, \mathcal{W}) = [k_0(\mathbf{w}, \mathbf{w}^{(1)}),$   
 185  $k_0(\mathbf{w}, \mathbf{w}^{(2)}), \dots, k_0(\mathbf{w}, \mathbf{w}^{(n)})]^\top$  is the covariance vector between  $\mathbf{w}$  and  $\mathcal{W}$ ;  $\mathbf{k}_0(\mathbf{w}', \mathcal{W}) = [k_0(\mathbf{w}', \mathbf{w}^{(1)}),$   
 186  $k_0(\mathbf{w}', \mathbf{w}^{(2)}), \dots, k_0(\mathbf{w}', \mathbf{w}^{(n)})]^\top$  is the covariance vector between  $\mathbf{w}'$  and  $\mathcal{W}$ ;  $\mathbf{K}_0$  is the covariance matrix  
 187 of  $\mathcal{W}$  with entry  $[\mathbf{K}_0]_{ij} = k_0(\mathbf{w}^{(i)}, \mathbf{w}^{(j)})$ .

### 188 3.3.1. Bayesian inference of REF

189 As an extended result of BPI [58], the posterior distribution of REF (denoted as  $\hat{\mathcal{M}}(\mathbf{v})$ ), i.e., integrating  
 190  $\hat{\mathcal{G}}(\mathbf{w})$  with respect to  $\mathbf{u}$  under the Gaussian weight  $f_{\mathcal{U}}(\mathbf{u})$ , still follows a GP. By repeated application  
 191 of Fubini's theorem, one can derive the analytical expressions of the posterior mean function  $\mu_{\hat{\mathcal{M}}}(\mathbf{v})$  and  
 192 posterior variance function  $\sigma_{\hat{\mathcal{M}}}^2(\mathbf{v})$  such that:

$$\mu_{\hat{\mathcal{M}}}(\mathbf{v}) = \mathbb{E}_{\mathcal{D}} [\hat{\mathcal{M}}(\mathbf{v})] = \Pi_{\mathbf{u}} [\mu_0(\mathbf{w})] + \Pi_{\mathbf{u}} [\mathbf{k}_0(\mathbf{w}, \mathcal{W})^\top] \mathbf{K}_0^{-1} (\mathcal{Z} - \boldsymbol{\mu}_0(\mathcal{W})), \quad (8)$$

$$\sigma_{\hat{\mathcal{M}}}^2(\mathbf{v}) = \mathbb{V}_{\mathcal{D}} [\hat{\mathcal{M}}(\mathbf{v})] = \Pi_{\mathbf{u}} \Pi_{\mathbf{u}'} [k_0(\mathbf{w}, (\mathbf{u}', \mathbf{v}))] - \Pi_{\mathbf{u}} [\mathbf{k}_0(\mathbf{w}, \mathcal{W})^\top] \mathbf{K}_0^{-1} \Pi_{\mathbf{u}} [\mathbf{k}_0(\mathbf{w}, \mathcal{W})], \quad (9)$$

194 where  $\mathbb{E}_{\mathcal{D}} [\cdot]$  and  $\mathbb{V}_{\mathcal{D}} [\cdot]$  refer to the expectation and variance operators taken with respect to the posterior  
 195 distributions of their arguments given data  $\mathcal{D}$ ;  $\Pi_{\mathbf{u}} [\cdot]$  denotes the integral operator taken with respect to  $\mathbf{u}$   
 196 under Gaussian weight  $f_{\mathcal{U}}(\mathbf{u})$ ;  $\Pi_{\mathbf{u}'} [\cdot]$  is similarly defined;  $\Pi_{\mathbf{u}} \Pi_{\mathbf{u}'} [\cdot]$  is the integral operator taken respect to  
 197 both  $\mathbf{u}$  and  $\mathbf{u}'$  under Gaussian weights  $f_{\mathcal{U}}(\mathbf{u})$  and  $f_{\mathcal{U}}(\mathbf{u}')$ ; The term  $\Pi_{\mathbf{u}} [\mu_0(\mathbf{w})]$  can be easily obtained as  
 198  $\Pi_{\mathbf{u}} [\mu_0(\mathbf{w})] = \beta$ ; The other terms can be derived as:

$$\Pi_{\mathbf{u}} [\mathbf{k}_0(\mathbf{w}, \mathcal{W})] = s_0^2 |\boldsymbol{\Sigma}_{\mathbf{u}}^{-1} + \mathbf{I}|^{-1/2} \exp \left[ -\frac{1}{2} \text{diag} \left\{ \mathcal{U} (\boldsymbol{\Sigma}_{\mathbf{u}} + \mathbf{I})^{-1} \mathcal{U}^\top - (\mathbf{v} - \boldsymbol{\nu}) \boldsymbol{\Sigma}_{\mathbf{v}}^{-1} (\mathbf{v} - \boldsymbol{\nu})^\top \right\} \right], \quad (10)$$

$$\Pi_{\mathbf{u}} \Pi_{\mathbf{u}'} [k_0(\mathbf{w}, \mathbf{w}')] = s_0^2 |2\boldsymbol{\Sigma}_{\mathbf{u}}^{-1} + \mathbf{I}|^{-1/2}, \quad (11)$$

200 where  $|\cdot|$  means the determinant of its argument;  $\mathbf{I}$  is a identity matrix of size  $d_1$ .

201 Note that the expressions for  $\mu_{\hat{\mathcal{M}}}(\mathbf{v})$  and  $\sigma_{\hat{\mathcal{M}}}^2(\mathbf{v})$  are similar in form to those of NIPI and CABO, but  
 202 essentially different due to the fact that the proposed method is established on the basis of the joint space  
 203 of standard normal variables and standard interval variables, while both NIPI and CABO are cast in the  
 204 standard normal space. The posterior mean function  $\mu_{\mathcal{M},n}(\mathbf{v})$  can be used as an estimate of  $\mathcal{M}(\mathbf{v})$  and  
 205 the posterior variance function  $\sigma_{\hat{\mathcal{M}}}^2(\mathbf{v})$  measures our uncertainty of the estimate after  $n$  observations have  
 206 been available. By using the linear transformation, one can easily obtain the posterior mean function  
 207  $\mu_{\hat{m}}(\boldsymbol{\alpha}) = \mu_{\hat{\mathcal{M}}}(T_2(\boldsymbol{\alpha}))$  and posterior variance function  $\sigma_{\hat{m}}^2(\boldsymbol{\alpha}) = \sigma_{\hat{\mathcal{M}}}^2(T_2(\boldsymbol{\alpha}))$  for  $\hat{m}(\boldsymbol{\alpha})$ .

### 208 3.3.2. Bayesian inference of RS-HDMR component functions of REF

209 In addition to the REF  $\hat{m}(\boldsymbol{\alpha})$ , the analyst may also be concerned about, e.g., identifying key variables  
 210 among  $\mathbf{A}$  that are more important for  $m(\boldsymbol{\alpha})$ . For this propose, the RS-HDMR is first employed to express

211  $\mathcal{M}(\mathbf{v})$  as the summation of a set of component functions with increasing dimensions [59]:

$$\mathcal{M}(\mathbf{v}) = \mathcal{M}_0 + \sum_{i=1}^{d_2} \mathcal{M}_i(v_i) + \sum_{1 \leq i < j \leq d_2} \mathcal{M}_{ij}(v_i, v_j) + \cdots + \mathcal{M}_{ij \dots d_2}(v_1, v_2, \dots, v_{d_2}), \quad (12)$$

212 where the zeroth-order component function  $\mathcal{M}_0$  is a constant representing the average value of  $\mathcal{M}(\mathbf{v})$  over  
 213 the entire domain  $\mathcal{V}$ , the first-order component function  $\mathcal{M}_i(v_i)$  represents the independent contribution of  
 214  $v_i$  acting alone to  $\mathcal{M}(\mathbf{v})$ , the second-order component function  $\mathcal{M}_{ij}(v_i, v_j)$  denotes the cooperative effects of  
 215  $v_i$  and  $v_j$  upon  $\mathcal{M}(\mathbf{v})$ , etc. The last term  $\mathcal{M}_{ij \dots d_2}(v_1, v_2, \dots, v_{d_2})$  describes any residual cooperative effects  
 216 of all input variables acting together to influence  $\mathcal{M}(\mathbf{v})$ . The component functions up to the second-order  
 217 can be defined as:

$$\mathcal{M}_0 = \int_{\mathcal{V}} \mathcal{M}(\mathbf{v}) d\mathbf{v} = \int_{\mathcal{V}} \int_{\mathcal{U}} \mathcal{G}(\mathbf{w}) f_{\mathcal{U}}(\mathbf{u}) d\mathbf{u} d\mathbf{v}, \quad (13)$$

$$\mathcal{M}_i(v_i) = \int_{\mathcal{V}_{-i}} \mathcal{M}(\mathbf{v}) d\mathbf{v}_{-i} - \mathcal{M}_0 = \int_{\mathcal{V}_{-i}} \int_{\mathcal{U}} \mathcal{G}(\mathbf{w}) f_{\mathcal{U}}(\mathbf{u}) d\mathbf{u} d\mathbf{v}_{-i} - \mathcal{M}_0, \quad (14)$$

$$\mathcal{M}_{ij}(v_i, v_j) = \int_{\mathcal{V}_{-ij}} \mathcal{M}(\mathbf{v}) d\mathbf{v}_{-ij} - \mathcal{M}_i(v_i) - \mathcal{M}_j(v_j) - \mathcal{M}_0 = \int_{\mathcal{V}_{-ij}} \int_{\mathcal{U}} \mathcal{G}(\mathbf{w}) f_{\mathcal{U}}(\mathbf{u}) d\mathbf{u} d\mathbf{v}_{-ij} - \mathcal{M}_i(v_i) - \mathcal{M}_j(v_j) - \mathcal{M}_0, \quad (15)$$

220 where  $\mathcal{V}_{-i}$  and  $\mathbf{v}_{-i}$  denote the space  $\mathcal{V}$  and the vector  $\mathbf{v}$  excluding the  $i$ -th dimension, respectively;  $\mathcal{V}_{-ij}$   
 221 and  $\mathbf{v}_{-ij}$  are similarly defined.

222 **As high-order component functions have small contributions for many realistic systems, the second-order**  
 223 **truncated RS-HDMR expansion is often considered [36, 40]. For this reason, only the component functions up**  
 224 **to the second-order are provided in the following via Bayesian inference. If necessary, high-order component**  
 225 **functions can also be derived similarly.**

226 *Zeroth-order RS-HDMR component.* As defined in Eq. (13), the zeroth-order RS-HDMR component  $\mathcal{M}_0$   
 227 is actually an integral of  $\mathcal{G}(\mathbf{w})$  with respect to  $\mathbf{w}$ . From a Bayesian quadrature perspective, the posterior  
 228 distribution of  $\mathcal{M}_0$  (denoted as  $\hat{\mathcal{M}}_0$ ) is Gaussian with posterior mean  $\mu_{\hat{\mathcal{M}}_0}$  and posterior variance  $\sigma_{\hat{\mathcal{M}}_0}^2$ ,  
 229 being:

$$\mu_{\hat{\mathcal{M}}_0} = \mathbb{E}_{\mathcal{D}} [\hat{\mathcal{M}}_0] = \Pi_{\mathbf{w}} [\mu_0(\mathbf{w})] + \Pi_{\mathbf{w}} [\mathbf{k}_0(\mathbf{w}, \mathcal{W})^T] \mathbf{K}_0^{-1} (\mathcal{Z} - \mu_0(\mathcal{W})), \quad (16)$$

$$\sigma_{\hat{\mathcal{M}}_0}^2 = \mathbb{V}_{\mathcal{D}} [\hat{\mathcal{M}}_0] = \Pi_{\mathbf{w}} \Pi_{\mathbf{w}'} [k_0(\mathbf{w}, \mathbf{w}')] - \Pi_{\mathbf{w}} [\mathbf{k}_0(\mathbf{w}, \mathcal{W})^T] \mathbf{K}_0^{-1} \Pi_{\mathbf{w}'} [\mathbf{k}_0(\mathbf{w}', \mathcal{W})], \quad (17)$$

231 where  $\Pi_{\mathbf{w}} [\mu_0(\mathbf{w})] = \beta$ , and other terms can be derived as:

$$\begin{aligned} \Pi_{\mathbf{w}} [\mathbf{k}_0(\mathbf{w}, \mathcal{W})] &= \Pi_{\mathbf{w}'} [\mathbf{k}_0(\mathbf{w}', \mathcal{W})] \\ &= s_0^2 |\boldsymbol{\Sigma}_{\mathbf{u}}^{-1} + \mathbf{I}|^{-1/2} \exp \left[ -\frac{1}{2} \text{diag} \left\{ \mathcal{U} (\boldsymbol{\Sigma}_{\mathbf{u}} + \mathbf{I})^{-1} \mathcal{U}^T \right\} \right] \\ &\quad \cdot \left( \frac{\pi}{2} \right)^{d_2/2} \text{prod}_2 \left\{ \left[ \text{erf} \left( (1 - \boldsymbol{\nu}) (2\boldsymbol{\Sigma}_{\mathbf{v}})^{-1/2} \right) - \text{erf} \left( -\boldsymbol{\nu} (2\boldsymbol{\Sigma}_{\mathbf{v}})^{-1/2} \right) \right] \boldsymbol{\Sigma}_{\mathbf{v}}^{1/2} \right\}, \end{aligned} \quad (18)$$



232

$$\begin{aligned} \Pi_{\mathbf{w}} \Pi_{\mathbf{w}'} [k_0(\mathbf{w}, \mathbf{w}')] = & s_0^2 |2\boldsymbol{\Sigma}_{\mathbf{u}}^{-1} + \mathbf{I}|^{-1/2} \\ & \cdot 2^{d_2} \text{prod}_1 \left\{ \text{diag} \left\{ \boldsymbol{\Sigma}_{\mathbf{v}} \left[ -1 + \exp \left[ -(2\boldsymbol{\Sigma}_{\mathbf{v}})^{-1} \right] + (2\pi^{-1} \boldsymbol{\Sigma}_{\mathbf{v}})^{-1/2} \text{erf} \left( (2\boldsymbol{\Sigma}_{\mathbf{v}})^{-1/2} \right) \right] \right\} \right\}, \end{aligned} \quad (19)$$

233 where  $\text{prod}_1 \{\cdot\}$  means to return the product of the elements of its argument;  $\text{prod}_2 \{\cdot\}$  is to get a column  
 234 vector containing the products of each row of its argument;  $\text{erf}(\cdot)$  stands for the error function. Note that  
 235 in Eq. (18) the argument in  $\text{prod}_2 \{\cdot\}$  is an  $n$ -by- $d_2$  matrix, while in Eq. (19) the argument in  $\text{prod}_1 \{\cdot\}$  is  
 236 a  $d_2$ -by-1 vector.

237 *First-order RS-HDMR component.* The first-order RS-HDMR component function  $\mathcal{M}_i(v_i)$  defined in Eq.  
 238 (14) is an integral (i.e., integrating  $\mathcal{G}(\mathbf{w})$  with respect to  $\mathbf{w}$  excluding  $v_i$ ) minus  $\mathcal{M}_0$ , and thus its posterior  
 239 distribution  $\hat{\mathcal{M}}_i(v_i)$  should follow a one-dimensional GP.

240 The posterior mean function  $\mu_{\hat{\mathcal{M}}_i}(v_i)$  of the first-order RS-HDMR component function  $\hat{\mathcal{M}}_i(v_i)$  can be  
 241 expressed as:

$$\mu_{\hat{\mathcal{M}}_i}(v_i) = \mathbb{E}_{\mathcal{D}} \left[ \hat{\mathcal{M}}_i(v_i) \right] = \Pi_{-v_i} [\mu_0(\mathbf{w})] + \Pi_{-v_i} \left[ \mathbf{k}_0(\mathbf{w}, \mathcal{W})^{\text{T}} \right] \mathbf{K}_0^{-1} (\boldsymbol{\mathcal{Z}} - \boldsymbol{\mu}_0(\mathcal{W})) - \mu_{\hat{\mathcal{M}}_0}, \quad (20)$$

242 where  $\Pi_{-v_i} [\cdot]$  denotes the integration of its argument taken over  $\mathbf{w}$  except  $v_i$ ; it is obvious that  $\Pi_{-v_i} [\mu_0(\mathbf{w})] =$   
 243  $\beta$ ; the term  $\Pi_{-v_i} [\mathbf{k}_0(\mathbf{w}, \mathcal{W})]$  can be derived as:

$$\begin{aligned} \Pi_{-v_i} [\mathbf{k}_0(\mathbf{w}, \mathcal{W})] = & s_0^2 |\boldsymbol{\Sigma}_{\mathbf{u}}^{-1} + \mathbf{I}|^{-1/2} \exp \left[ -\frac{1}{2} \text{diag} \left\{ \mathbf{U} (\boldsymbol{\Sigma}_{\mathbf{u}} + \mathbf{I})^{-1} \mathbf{U}^{\text{T}} \right\} \right] \\ & \cdot \left( \frac{\pi}{2} \right)^{(d_2-1)/2} \text{prod}_2 \left\{ \left[ \text{erf} \left( (1 - \boldsymbol{\nu}_{-,i}) (2\boldsymbol{\Sigma}_{\mathbf{v}_{-i}})^{-1/2} \right) - \text{erf} \left( -\boldsymbol{\nu}_{-,i} (2\boldsymbol{\Sigma}_{\mathbf{v}_{-i}})^{-1/2} \right) \right] \boldsymbol{\Sigma}_{\mathbf{v}_{-i}}^{1/2} \right\} \\ & \cdot \exp \left[ -\frac{1}{2} \text{diag} \left\{ - (v_i - \boldsymbol{\nu}_{,i}) \boldsymbol{\Sigma}_{\mathbf{v}_i}^{-1} (v_i - \boldsymbol{\nu}_{,i})^{\text{T}} \right\} \right], \end{aligned} \quad (21)$$

244 in which  $\boldsymbol{\nu}_{,i}$  is the  $i$ -th column of  $\boldsymbol{\nu}$ ,  $\boldsymbol{\nu}_{-,i}$  represents the matrix generated by removing  $\boldsymbol{\nu}_{,i}$  from  $\boldsymbol{\nu}$ ,  $\boldsymbol{\Sigma}_{\mathbf{v}_i}$   
 245 denotes the  $(i, i)$ -th element of  $\boldsymbol{\Sigma}_{\mathbf{v}}$ , and  $\boldsymbol{\Sigma}_{\mathbf{v}_{-i}}$  stands for the matrix generated by removing the  $i$ -th column  
 246 and  $i$ -th row of  $\boldsymbol{\Sigma}_{\mathbf{v}}$ .

247 For the posterior variance function  $\sigma_{\hat{\mathcal{M}}_i}^2(v_i)$  of the first-order RS-HDMR component function  $\hat{\mathcal{M}}_i(v_i)$ ,  
 248 one can refer to [Appendix A](#).

249 *Second-order RS-HDMR component.* Similarly, the second-order RS-HDMR component function  $\mathcal{M}_{ij}(v_i, v_j)$   
 250 defined in Eq. (15) is an integral (i.e., integrating  $\mathcal{G}(\mathbf{w})$  with respect to  $\mathbf{w}$  excluding  $v_i$  and  $v_j$ ) **diminished**  
 251 **by**  $\mathcal{M}_i(v_i)$ ,  $\mathcal{M}_j(v_j)$  and  $\mathcal{M}_0$ , and thus its posterior distribution  $\hat{\mathcal{M}}_{ij}(v_i, v_j)$  should follow a two-dimensional  
 252 GP.

253 The posterior mean function  $\mu_{\hat{\mathcal{M}}_{ij}}(v_i, v_j)$  of the first-order RS-HDMR component function  $\hat{\mathcal{M}}_{ij}(v_i, v_j)$

254 can be given by:

$$\begin{aligned} \mu_{\hat{\mathcal{M}}_{ij}}(v_i, v_j) &= \mathbb{E}_{\mathcal{D}} \left[ \hat{\mathcal{M}}_{ij}(v_i, v_j) \right] \\ &= \Pi_{-\mathbf{v}_{ij}} [\mu_0(\mathbf{w})] + \Pi_{-\mathbf{v}_{ij}} \left[ \mathbf{k}_0(\mathbf{w}, \mathcal{W})^\top \right] \mathbf{K}_0^{-1} (\mathcal{Z} - \boldsymbol{\mu}_0(\mathcal{W})) - \mu_{\hat{\mathcal{M}}_i}(v_i) - \mu_{\hat{\mathcal{M}}_j}(v_j) - \mu_{\hat{\mathcal{M}}_0}, \end{aligned} \quad (22)$$

255 where the term  $\Pi_{-\mathbf{v}_{ij}} [\mu_0(\mathbf{w})]$  is equal to  $\beta$ , and the term  $\Pi_{-\mathbf{v}_{ij}} [\mathbf{k}_0(\mathbf{w}, \mathcal{W})]$  is derived as:

$$\begin{aligned} \Pi_{-\mathbf{v}_{ij}} [\mathbf{k}_0(\mathbf{w}, \mathcal{W})] &= s_0^2 |\boldsymbol{\Sigma}_{\mathbf{u}}^{-1} + \mathbf{I}|^{-1/2} \exp \left[ -\frac{1}{2} \text{diag} \left\{ \mathcal{U} (\boldsymbol{\Sigma}_{\mathbf{u}} + \mathbf{I})^{-1} \mathcal{U}^\top \right\} \right] \\ &\quad \cdot \left( \frac{\pi}{2} \right)^{(d_2-2)/2} \text{prod}_2 \left\{ \left[ \text{erf} \left( (1 - \mathbf{v}_{,-ij}) (2\boldsymbol{\Sigma}_{\mathbf{v}_{-ij}})^{-1/2} \right) - \text{erf} \left( -\mathbf{v}_{,-ij} (2\boldsymbol{\Sigma}_{\mathbf{v}_{-ij}})^{-1/2} \right) \right] \boldsymbol{\Sigma}_{\mathbf{v}_{-ij}}^{1/2} \right\} \\ &\quad \cdot \exp \left[ -\frac{1}{2} \text{diag} \left\{ - (v_{ij} - \mathbf{v}_{,ij}) \boldsymbol{\Sigma}_{\mathbf{v}_{ij}}^{-1} (v_{ij} - \mathbf{v}_{,ij})^\top \right\} \right]. \end{aligned} \quad (23)$$

256 For the posterior variance function  $\sigma_{\hat{\mathcal{M}}_{ij}}^2(v_i, v_j)$  of the second-order RS-HDMR component function  
257  $\hat{\mathcal{M}}_{ij}(v_i, v_j)$ , one can refer to [Appendix B](#). ■

258 One should note that the above results are essentially different from those in NIPI. Once these RS-HDMR  
259 component functions of  $\hat{\mathcal{M}}(\mathbf{v})$  are properly inferred, they can be transformed by a linear transformation to  
260 yield the RS-HDMR component functions for  $\hat{m}(\boldsymbol{\alpha})$ .

### 261 3.3.3. Bayesian inference of extrema of REF

262 If we stop after obtaining  $n$  observations of the  $\mathcal{G}$ -function, a risk-neutral choice for the minimum or  
263 maximum of the REF would be the minimum or maximum of the posterior mean function  $\mu_{\hat{m}}(\boldsymbol{\alpha})$ . As  
264  $\mu_{\hat{m}}(\boldsymbol{\alpha})$  has been derived in a closed-form, the extrema of the REF can be inferred from  $\mu_{\hat{m}}(\boldsymbol{\alpha})$  by simply  
265 applying a global optimization algorithm such that:

$$\hat{m}_l = \min_{\boldsymbol{\alpha} \in [\underline{\boldsymbol{\alpha}}, \bar{\boldsymbol{\alpha}}]} \mu_{\hat{m}}(\boldsymbol{\alpha}), \quad (24)$$

$$\hat{m}_u = \max_{\boldsymbol{\alpha} \in [\underline{\boldsymbol{\alpha}}, \bar{\boldsymbol{\alpha}}]} \mu_{\hat{m}}(\boldsymbol{\alpha}). \quad (25)$$

267 Besides, since the posterior variance function  $\sigma_{\hat{m}}^2(\boldsymbol{\alpha})$  is also available, the prediction errors regarding the  
268 minimum and maximum estimators in Eqs. (24) and (25) can be measured by the posterior variances:

$$\text{Var} [\hat{m}_l] = \sigma_{\hat{m}}^2(\boldsymbol{\alpha}^-), \quad (26)$$

$$\text{Var} [\hat{m}_u] = \sigma_{\hat{m}}^2(\boldsymbol{\alpha}^+), \quad (27)$$

270 where  $\boldsymbol{\alpha}^- = \arg \min_{\boldsymbol{\alpha} \in [\underline{\boldsymbol{\alpha}}, \bar{\boldsymbol{\alpha}}]} \mu_{\hat{m}}(\boldsymbol{\alpha})$  and  $\boldsymbol{\alpha}^+ = \arg \max_{\boldsymbol{\alpha} \in [\underline{\boldsymbol{\alpha}}, \bar{\boldsymbol{\alpha}}]} \mu_{\hat{m}}(\boldsymbol{\alpha})$  are the minimum point and maximum  
271 point, respectively.

272 *3.4. Parallel Bayesian experimental design*

273 Another significant advantage of the above framework is that it offers the possibility for incorporating  
 274 our prior knowledge and developing a Bayesian experimental design strategy. This advantage is also realized  
 275 in both NIPI and CABO. These two methods, however, are in a pure sequential manner to acquire the  $\mathcal{G}$ -  
 276 function. That is, at each iteration only one point is allowed to be selected and a single  $\mathcal{G}$ -function evaluation  
 277 is subsequently performed. The sequential experimental strategies would be less efficient and flexible when  
 278 parallel computing architectures are available. Besides, the one for NIPI is specifically designed for inferring  
 279 RS-HDMR component functions, whereas the one for CABO is only developed for inferring the extrema  
 280 of the REF. Based on these considerations, a novel contribution here is to present a **multi-point** selection  
 281 criterion that can support parallel evaluations of the  $\mathcal{G}$ -function and also enable us to estimate the REF, its  
 282 RS-HDMR component functions and bounds at the same time. In this study, the preferred number of CPU  
 283 cores or workers in a parallel pool is assumed to be an even number, denoted by  $c$ .

284 *Stage 1: Global improvement.* Supposing that we have only obtained a small set of initial observations,  
 285 the first stage of our strategy aims to improve the global accuracy of the REF. The key lies in three main  
 286 aspects: (1) how can we measure the global accuracy of the REF? (2) how to select  $c$  points at each iteration  
 287 that are expected to improve the global accuracy of the REF? (3) when to stop the iteration at this stage?

288 As the zero-th order RS-HDMR component  $\mathcal{M}_0$  is defined as an integral of the REF  $\mathcal{M}(\mathbf{v})$  with respect  
 289 to  $\mathbf{v}$  (called augmented expectation), its accuracy may reflect the global accuracy of the REF to some  
 290 extent. Therefore, the accuracy of  $\hat{\mathcal{M}}_0$  is taken as a global accuracy measure of  $\hat{\mathcal{M}}(\mathbf{v})$  in this study, which  
 291 can be quantified by the posterior variance  $\sigma_{\hat{\mathcal{M}}_0}^2$ . Inspired by [23, 40, 41], a new acquisition function, called  
 292 posterior variance contribution to the augmented expectation (denoted as  $\text{PVC}^A$ ), is given by:

$$\text{PVC}^A(\mathbf{w}) = \Pi_{\mathbf{w}'} [k_n(\mathbf{w}, \mathbf{w}')] \times f_{\mathcal{W}}(\mathbf{w}) = \left\{ \Pi_{\mathbf{w}'} [k_0(\mathbf{w}, \mathbf{w}')] - \mathbf{k}_0(\mathbf{w}, \mathcal{W})^T \mathbf{K}_0^{-1} \Pi_{\mathbf{w}'} [\mathbf{k}_0(\mathbf{w}', \mathcal{W})] \right\} \times f_{\mathcal{W}}(\mathbf{w}), \quad (28)$$

293 where the closed-form expression of  $\Pi_{\mathbf{w}'} [\mathbf{k}_0(\mathbf{w}', \mathcal{W})]$  has been given in Eq. (18); Similarly, the term  
 294  $\Pi_{\mathbf{w}'} [k_0(\mathbf{w}, \mathbf{w}')] can be derived as:$

$$\begin{aligned} \Pi_{\mathbf{w}'} [k_0(\mathbf{w}, \mathbf{w}')] = & s_0^2 |\boldsymbol{\Sigma}_{\mathbf{u}}^{-1} + \mathbf{I}|^{-1/2} \exp \left[ -\frac{1}{2} \text{diag} \left\{ \mathbf{u} (\boldsymbol{\Sigma}_{\mathbf{u}} + \mathbf{I})^{-1} \mathbf{u}^T \right\} \right] \\ & \cdot \left( \frac{\pi}{2} \right)^{d_2/2} \text{prod}_2 \left\{ \left[ \text{erf} \left( (1 - \mathbf{v}) (2\boldsymbol{\Sigma}_{\mathbf{v}})^{-1/2} \right) - \text{erf} \left( -\mathbf{v} (2\boldsymbol{\Sigma}_{\mathbf{v}})^{-1/2} \right) \right] \boldsymbol{\Sigma}_{\mathbf{v}}^{1/2} \right\}. \end{aligned} \quad (29)$$

295 **The acquisition function in Eq. (28) is said to be ‘new’ because it is essentially not the same as those**  
 296 **in the cited references.** It should be noted that  $\sigma_{\hat{\mathcal{M}}_0}^2 = \int_{\mathcal{W}} \text{PVC}^A(\mathbf{w}) d\mathbf{w}$  holds, which implies that the  
 297  $\text{PVC}^A$  function can measure the contribution of our epistemic uncertainty at  $\mathbf{w}$  to  $\sigma_{\hat{\mathcal{M}}_0}^2$ . For this reason, by  
 298 selecting  $\mathbf{w}^{(n+1)} = \arg \max_{\mathbf{w} \in \mathcal{W}} \text{PVC}^A(\mathbf{w})$  as the best next point to evaluate the  $\mathcal{G}$ -function, it is expected  
 299 that the posterior variance of the augmented expectation will decrease the most, and hence the accuracy of

300 the posterior mean of the augmented expectation will be improved the most. However, adding one single  
 301 point at a time **may waste other useful information** and cannot allow to make use of parallelization, and  
 302 hence it could be inefficient especially when parallel evaluations are possible.

303 In this study, we propose a novel strategy to parallelize the developed PBQO method by providing  $c$   
 304 points at each iteration. This strategy is motivated by the fact that the  $\text{PVC}^{\text{A}}$  function (defined in Eq.  
 305 (28)) only explicitly depends on the sampled locations, not on function values at these points. For this  
 306 reason, we can rewrite the  $\text{PVC}^{\text{A}}$  function as  $\text{PVC}^{\text{A}}(\mathbf{w}, \mathcal{W})$ . Therefore, it is possible to select  $c$  points  
 307 ahead of observing their  $\mathcal{G}$ -function values based on the  $\text{PVC}^{\text{A}}(\mathbf{w}, \mathcal{W})$  function. Specifically, each point  
 308 can be selected sequentially, with the  $\text{PVC}^{\text{A}}$  function modified by considering the newly selected points at  
 309 the current iteration. **The assumption behind this strategy is that the hyper-parameters will not change,**  
 310 **and hence the  $\text{PVC}^{\text{A}}$  function remains the same during the process of identifying the next  $c - 1$  points.**  
 311 **In fact, the hyper-parameters do change if we update immediately the GP after each point is chosen and**  
 312 **its  $\mathcal{G}$ -function value is computed, which, however, corresponds to the single-point selection strategy. Our**  
 313 **idea is expected to work since the hyper-parameters may not vary too much within the next few steps.**  
 314 The pseudocode of the proposed multi-point selection strategy is given in Algorithm 1. Until  $c$  points are  
 315 obtained, evaluating the  $\mathcal{G}$ -function at these points can be run in parallel, and the GP model can be updated  
 316 subsequently. This iteration process is repeated until a stopping criterion is reached, which is defined as  
 317 the posterior coefficient of variation (COV) of the augmented expectation less than a pre-specified tolerance  
 318  $\varepsilon^{\text{BPI}}$ , i.e.,  $\frac{\sigma_{\mathcal{M}_0}}{|\mu_{\mathcal{M}_0}|} < \varepsilon^{\text{BPI}}$ . To avoid possible premature convergence, the stopping criterion is required to  
 319 be satisfied several (e.g., two) times in successive iterations. It should be noted that the proposed multi-  
 320 point selection strategy is computationally inexpensive and can usually produce a batch of  $c$  diverse points  
 321 according to our computational experience, which are thus effective and informative for parallelization.

---

**Algorithm 1** Proposed multi-point selection strategy based on the  $\text{PVC}^{\text{A}}(\mathbf{w}, \mathcal{W})$  function

---

- 1: **Input:**  $c$  and  $\text{PVC}^{\text{A}}(\mathbf{w}, \mathcal{W})$
  - 2: **for**  $i = 1 \rightarrow c$  **do**
  - 3:      $\mathbf{w}^{(n+i)} = \arg \max_{\mathbf{w} \in \mathcal{W}} \text{PVC}^{\text{A}}(\mathbf{w}, \mathcal{W})$
  - 4:      $\mathcal{W} = \mathcal{W} \cup \mathbf{w}^{(n+i)}$
  - 5: **end for**
  - 6: **Output:**  $\mathbf{w}^{(n+1)}, \mathbf{w}^{(n+2)}, \dots, \mathbf{w}^{(n+c)}$
- 

322 *Stage 2: Local improvement.* After stage 1, it is expected that the general trend of the REF has been  
 323 captured. However, the local features of the REF, e.g., minimum and maximum, may still be inaccurate.  
 324 In this regard, the second stage of our strategy attempts to further improve the accuracy of the resulting  
 325 REF from stage 1, with special emphasis on its extrema.

326 As the posterior distribution of the REF follows a GP, the expected improvement criterion originally  
 327 introduced in BGO [56] could be adopted for our purposes. Let  $\hat{\mathcal{M}}_l(\mathbf{v}^-)$  denote the current minimum, and  
 328  $\mathbf{v}^-$  the minimum point, i.e.,  $\mathbf{v}^- = \arg \min_{\mathbf{v} \in \mathcal{V}} \mu_{\hat{\mathcal{M}}}(\mathbf{v})$ . The improvement for the current minimum at the  
 329 point  $\mathbf{v}$  can be defined as  $I(\mathbf{v}) = \max(\hat{\mathcal{M}}_l(\mathbf{v}^-) - \mu_{\hat{\mathcal{M}}}(\mathbf{v}), 0)$ . The acquisition function, called expected  
 330 improvement for the minimization (abbreviated as  $\text{EI}^{\text{MIN}}$ ), is to simply take the expected value of  $I(\mathbf{v})$ , i.e.,  
 331  $\text{EI}^{\text{MIN}}(\mathbf{v}) = \mathbb{E}[I(\mathbf{v})]$ . The closed-form expression of  $\text{EI}^{\text{MIN}}$  can be written as [56]:

$$\text{EI}^{\text{MIN}}(\mathbf{v}) = \left( \hat{\mathcal{M}}_l(\mathbf{v}^-) - \mu_{\hat{\mathcal{M}}}(\mathbf{v}) \right) \Phi \left( \frac{\hat{\mathcal{M}}_l(\mathbf{v}^-) - \mu_{\hat{\mathcal{M}}}(\mathbf{v})}{\sigma_{\hat{\mathcal{M}}}(\mathbf{v})} \right) + \sigma_{\hat{\mathcal{M}}}(\mathbf{v}) \varphi \left( \frac{\hat{\mathcal{M}}_l(\mathbf{v}^-) - \mu_{\hat{\mathcal{M}}}(\mathbf{v})}{\sigma_{\hat{\mathcal{M}}}(\mathbf{v})} \right), \quad (30)$$

332 where  $\varphi(\cdot)$  and  $\Phi(\cdot)$  are the PDF and cumulative distribution function (CDF) of the standard normal  
 333 distribution, respectively. The  $\text{EI}^{\text{MIN}}$  function actually measures how much improvement for the minimum  
 334 is expected to achieve by sampling at  $\mathbf{v}$ . Thus, the next best point for  $\mathbf{v}$  can be selected by maximizing the  
 335  $\text{EI}^{\text{MIN}}$  function, i.e.,  $\underline{\mathbf{v}}^* = \arg \max_{\mathbf{v} \in \mathcal{V}} \text{EI}^{\text{MIN}}(\mathbf{v})$ . The first summation term in Eq. (30) is the exploitation  
 336 term encouraging to sample where  $\mu_{\hat{\mathcal{M}}}(\mathbf{v})$  is small, whereas the second summation term is the exploration  
 337 term encouraging to sample where  $\sigma_{\hat{\mathcal{M}}}(\mathbf{v})$  is large. At this stage, the associated stopping criterion can be  
 338 given as [60]:

$$\frac{|\max_{\mathbf{v} \in \mathcal{V}} \text{EI}^{\text{MIN}}(\mathbf{v})|}{\max \mathcal{Z} - \min \mathcal{Z}} < \varepsilon^{\text{BGO}}, \quad (31)$$

339 where  $\varepsilon^{\text{BGO}}$  is a user-defined tolerance. Similarly, the stopping criterion also needs to be met for two times  
 340 in succession. Once  $\underline{\mathbf{v}}^*$  is identified, the best next point for  $\mathbf{u}$  can also be specified. In order to improve  
 341 the accuracy of  $\mu_{\hat{\mathcal{M}}}(\underline{\mathbf{v}}^*)$ , an acquisition function measuring the posterior variance contribution to  $\sigma_{\hat{\mathcal{M}}}^2(\underline{\mathbf{v}}^*)$   
 342 (abbreviated as  $\text{PVC}^{\text{MIN}}$ ), can be defined:

$$\begin{aligned} \text{PVC}^{\text{MIN}}(\mathbf{u}) &= \Pi_{\mathbf{u}'} [k_n((\mathbf{u}, \underline{\mathbf{v}}^*), (\mathbf{u}', \underline{\mathbf{v}}^*))] \times f_{\mathcal{U}}(\mathbf{u}) \\ &= \left\{ \Pi_{\mathbf{u}'} [k_0((\mathbf{u}, \underline{\mathbf{v}}^*), (\mathbf{u}', \underline{\mathbf{v}}^*))] - \mathbf{k}_0((\mathbf{u}, \underline{\mathbf{v}}^*), \mathcal{W})^T \mathbf{K}_0^{-1} \Pi_{\mathbf{u}'} [k_0((\mathbf{u}', \underline{\mathbf{v}}^*), \mathcal{W})] \right\} \times f_{\mathcal{U}}(\mathbf{u}), \end{aligned} \quad (32)$$

343 where the term  $\Pi_{\mathbf{u}'} [k_0((\mathbf{u}', \underline{\mathbf{v}}^*), \mathcal{W})]$  can be generated as Eq. (10) by replacing  $\mathbf{v}$  by  $\underline{\mathbf{v}}^*$ , and the term  
 344  $\Pi_{\mathbf{u}'} [k_0((\mathbf{u}, \underline{\mathbf{v}}^*), (\mathbf{u}', \underline{\mathbf{v}}^*))]$  can be derived as:

$$\Pi_{\mathbf{u}'} [k_0((\mathbf{u}, \underline{\mathbf{v}}^*), (\mathbf{u}', \underline{\mathbf{v}}^*))] = s_0^2 |\boldsymbol{\Sigma}_{\mathbf{u}}^{-1} + \mathbf{I}|^{-1/2} \exp \left[ -\frac{1}{2} \text{diag} \left\{ \mathbf{u} (\boldsymbol{\Sigma}_{\mathbf{u}} + \mathbf{I})^{-1} \mathbf{u}^T \right\} \right]. \quad (33)$$

345 **In analogy** to  $\text{PVC}^{\text{A}}$  criterion (see Algorithm 1),  $c/2$  points for  $\mathbf{u}$  can be selected sequentially by maximizing  
 346 the  $\text{PVC}^{\text{MIN}}$  function, denoted as  $\underline{\mathbf{u}}^{(n+i)}$  ( $i = 1, 2, \dots, c/2$ ). The stopping criterion is defined as  $\frac{\sigma_{\hat{\mathcal{M}}}(\underline{\mathbf{v}}^*)}{|\mu_{\hat{\mathcal{M}}}(\underline{\mathbf{v}}^*)|} <$   
 347  $\varepsilon^{\text{BPI}}$ , which should be satisfied two times in succession. The identified points for  $\mathbf{w}$  can be simply formed  
 348 as:  $(\underline{\mathbf{u}}^{(n+1)}, \underline{\mathbf{v}}^*), (\underline{\mathbf{u}}^{(n+2)}, \underline{\mathbf{v}}^*), \dots, (\underline{\mathbf{u}}^{(n+c/2)}, \underline{\mathbf{v}}^*)$ .

349 Similar to Eqs. (30) and (32), the expected improvement and posterior variance contribution for maxi-  
 350 mization can also be defined, which are denoted as  $\text{EI}^{\text{MAX}}$  and  $\text{PVC}^{\text{MAX}}$ , respectively. To limit the paper  
 351 length, however, we will not give them in detail. The next point for  $\mathbf{v}$  can be determined by maximizing

352 the  $\text{EI}^{\text{MAX}}$  function, i.e.,  $\bar{\mathbf{v}}^* = \arg \max_{\mathbf{v} \in \mathcal{V}} \text{EI}^{\text{MAX}}(\mathbf{v})$ . Then, based on the  $\text{PVC}^{\text{MAX}}$  function, one can  
 353 sequentially identify  $c/2$  points for  $\mathbf{u}$ , denoted as  $\bar{\mathbf{u}}^{(n+i)}$  ( $i = 1, 2, \dots, c/2$ ). The remaining  $c/2$  points for  $\mathbf{w}$   
 354 can be generated as:  $(\bar{\mathbf{u}}^{(n+1)}, \bar{\mathbf{v}}^*), (\bar{\mathbf{u}}^{(n+2)}, \bar{\mathbf{v}}^*), \dots, (\bar{\mathbf{u}}^{(n+c/2)}, \bar{\mathbf{v}}^*)$

355 As a result, a total number of  $c$  points for  $\mathbf{w}$  can be obtained, and the corresponding  $\mathcal{G}$ -function values  
 356 can be computed at the same time by running on  $c$  cores simultaneously. After that, the GP model can be  
 357 updated based on the past observations. Once pre-defined stopping criteria are reached, these quantities of  
 358 interest can be extracted from the final GP model.

### 359 3.5. Numerical implementation of PBQO

360 For numerical implementation of the proposed PBQO method, the basic procedures are summarized as  
 361 follows, which are also illustrated by Fig. 1.

362

#### 363 **Step 1: Get initial observations**

364 The first step consists of generating a small set of  $n_0$  initial samples using Latin hypercube sampling  
 365 (LHS), denoted as  $\mathcal{W} = (\mathbf{U}, \mathcal{V}) = \{\mathbf{w}^{(j)}\}_{j=1}^{n_0}$ . The real  $\mathcal{G}$ -function is then evaluated at these points to obtain  
 366 corresponding observations, i.e.,  $\mathcal{Z} = \{z^{(i)} = \mathcal{G}(\mathbf{w}^{(i)})\}_{j=1}^{n_0}$ , which can be parallelized straightforwardly. The  
 367 initial training dataset can be constructed:  $\mathcal{D} = \{\mathcal{W}, \mathcal{Z}\}$ . Let  $n = n_0$ ;

368

#### 369 **Step 2: Train a GP model**

369 Based on data  $\mathcal{D}$ , train a new GP model  $\mathcal{GP}(\mu_n(\mathbf{w}), k_n(\mathbf{w}, \mathbf{w}'))$  for the  $\mathcal{G}$ -function. In this study, the  
 370 *fitrgp* function in Matlab Statistics and Machine Learning Toolbox is used. The prior mean function and  
 371 covariance function are specified as constant and squared exponential kernel, respectively.

372

#### 373 **Step 3: Check the stopping criterion**

373 From the trained GP model, one can compute the posterior mean  $\mu_{\hat{\mathcal{M}}_0}$  and posterior variance  $\sigma_{\hat{\mathcal{M}}_0}^2$  of  
 374 the augmented expectation by Eqs. (16) and (17), respectively. If the stopping criterion  $\frac{\sigma_{\hat{\mathcal{M}}_0}}{|\mu_{\hat{\mathcal{M}}_0}|} < \varepsilon^{\text{BPI}}$  is  
 375 satisfied two times in succession, go to **Step 5**; else, go to **Step 4**;

376

#### 377 **Step 4: Identify new observations by the $\text{PVC}^{\text{A}}$ criterion**

377 At this stage, one can identify  $c$  points for  $\mathbf{W}$  by sequentially maximizing the  $\text{PVC}^{\text{A}}$  function (Eq. (28)),  
 378 denoted as  $\mathcal{W}^* = \{\mathbf{w}^*\}_{j=1}^c$ . Then, these points are evaluated on the real  $\mathcal{G}$ -function in parallel to obtain  
 379 corresponding observations, which are denoted as  $\mathcal{Z}^* = \{z^*\}_{j=1}^c$ . At last, the training dataset  $\mathcal{D}$  can be  
 380 enriched with  $\mathcal{D}^* = \{\mathcal{W}^*, \mathcal{Z}^*\}$ . Let  $n = n + c$  and go to **Step 2**;

381

#### 382 **Step 5: Select new points by the quadruplet criteria**

382 The next best points  $\underline{\mathbf{v}}^*$  and  $\bar{\mathbf{v}}^*$  can be selected by  $\underline{\mathbf{v}}^* = \arg \max_{\mathbf{v} \in \mathcal{V}} \text{EI}^{\text{MIN}}(\mathbf{v})$  and  $\bar{\mathbf{v}}^* = \arg \max_{\mathbf{v} \in \mathcal{V}} \text{EI}^{\text{MAX}}(\mathbf{v})$ ,  
 383 respectively. Then, one can select  $c/2$  points  $(\underline{\mathbf{u}}^{(i)})$  ( $i = 1, 2, \dots, c/2$ ) and  $(\bar{\mathbf{u}}^{(i)})$  ( $i = 1, 2, \dots, c/2$ ) by sequen-  
 384 tially maximizing the  $\text{PVC}^{\text{MIN}}$  function and  $\text{PVC}^{\text{MAX}}$  function, respectively. For convenience, we denote the

385  $c/2$  points for minimization by  $\underline{\mathcal{W}} = \{(\mathbf{v}^*, \mathbf{u}^{(1)}), (\mathbf{v}^*, \mathbf{u}^{(2)}), \dots, (\mathbf{v}^*, \mathbf{u}^{(c/2)})\}$ ,  $c/2$  points for maximization  
 386 by  $\overline{\mathcal{W}} = \{(\overline{\mathbf{v}}^*, \overline{\mathbf{u}}^{(1)}), (\overline{\mathbf{v}}^*, \overline{\mathbf{u}}^{(2)}), \dots, (\overline{\mathbf{v}}^*, \overline{\mathbf{u}}^{(c/2)})\}$ , and  $\mathcal{W}^* = \{\underline{\mathcal{W}}, \overline{\mathcal{W}}\}$ ;

387 **Step 6: Judge the stopping criteria**

388 In this step, four stopping criteria should be judged, i.e.,  $\frac{|\max_{\mathbf{v} \in \mathcal{V}} \text{EI}^{\text{MIN}}(\mathbf{v})|}{\max \mathcal{Z} - \min \mathcal{Z}} < \varepsilon^{\text{BGO}}$ ,  $\frac{\sigma_{\mathcal{M}}(\mathbf{v}^*)}{|\mu_{\mathcal{M}}(\mathbf{v}^*)|} < \varepsilon^{\text{BPI}}$ ,  
 389  $\frac{|\max_{\mathbf{v} \in \mathcal{V}} \text{EI}^{\text{MAX}}(\mathbf{v})|}{\max \mathcal{Z} - \min \mathcal{Z}} < \varepsilon^{\text{BGO}}$  and  $\frac{\sigma_{\mathcal{M}}(\overline{\mathbf{v}}^*)}{|\mu_{\mathcal{M}}(\overline{\mathbf{v}}^*)|} < \varepsilon^{\text{BPI}}$ . If all these stopping criteria are met two times in succession,  
 390 go to **Step 9**; else, go to **Step 7**;

391 **Step 7: Obtain new observations by parallel computing**

392 Evaluation of the real  $\mathcal{G}$ -function at these  $c$  points  $\mathcal{W}^*$  from **Step 5** can be performed in parallel, and  
 393  $c$  observations are obtained  $\mathcal{Z}^* = \{z^*\}_{j=1}^c$ . Finally, the training dataset  $\mathcal{D}$  is updated with the new data  
 394  $\mathcal{D}^* = \{\mathcal{W}^*, \mathcal{Z}^*\}$ . Let  $n = n + c$ ;

395 **Step 8: Train a GP model**

396 Train a new GP model  $\mathcal{GP}(\mu_n(\mathbf{w}), k_n(\mathbf{w}, \mathbf{w}'))$  for the  $\mathcal{G}$ -function with data  $\mathcal{D}$ , and go to **Step 5**.

397 **Step 9: Return quantities of interest**

398 The posterior means and variances of these quantities of interest, such as REF, its RS-HDMR component  
 399 functions and bounds, can be extracted from the trained GP model. The posterior means can serve as  
 400 estimates for these quantities, and the posterior variances measure the epistemic uncertainties (numerical  
 401 errors) about our estimates.

402  
 403 To initialize the algorithm, there parameters  $n_0$ ,  $\varepsilon^{\text{BPI}}$  and  $\varepsilon^{\text{BGO}}$  need to be specified. The initial sam-  
 404 ple size  $n_0$  should not choose too large as we wish to enlarge the sample size sequentially. For the two  
 405 thresholds  $\varepsilon^{\text{BPI}}$  and  $\varepsilon^{\text{BGO}}$ , proper values are also important as they influence the accuracy and efficiency  
 406 of the proposed method. According to our experience,  $n_0$  can take values between 5 and 20 depending  
 407 on the complexity of the problem at hand, and  $\varepsilon^{\text{BPI}}$  and  $\varepsilon^{\text{BGO}}$  can be set in the orders of 0.01 and 0.001  
 408 respectively. Several optimization problems are involved in the implementation procedures, one can simply  
 409 use the global optimization algorithms (e.g., genetic algorithm) as the objective functions are all in closed  
 410 form.

411

### 412 3.6. Relationship to existing NIPI and CABO methods

413 The proposed PBQO method does share some similarities with the NIPI method and CABO method.  
 414 For example, they all rely on the use of the GP model in a Bayesian fashion, and can avoid nested loops.  
 415 However, the differences among the three methods are also significant on several main aspects:

- 416 a) The proposed PBQO method transforms the interval variables (including the interval variables in p-  
 417 boxes) into standard interval ones by a linear transformation. On the contrary, by assuming auxiliary

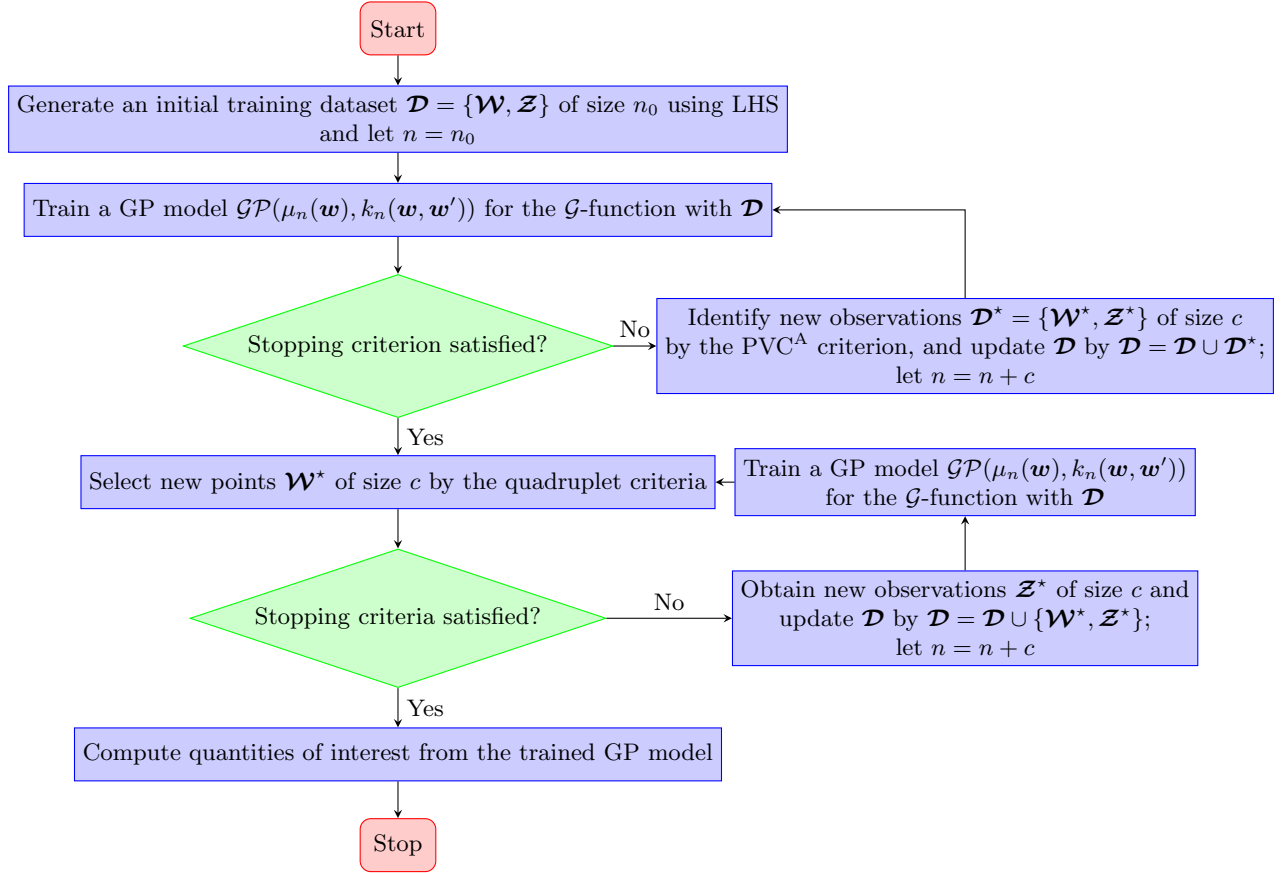


Figure 1: Flowchart of the proposed PBQO method.

418 uniform distributions for the interval variables, the NIPI and CABO methods convert the interval  
 419 variables to standard normal ones by a nonlinear transformation. In conjunction with the squared  
 420 exponential kernel, both of those two strategies can result in analytically tractable results for the REF  
 421 and its HS-HDMR. However, the NIPI and CABO methods introduce an additional assumption and  
 422 artificially added nonlinearity. More importantly, the transformation strategy for NIPI and CABO is  
 423 the cause of poor performance near the bounds of the interval variables. To mitigate this problem,  
 424 one needs to relax the support of the interval variables when applying NIPI and CABO;

425 b) Due to the differences in a), the posterior means and variances of the REF and its RS-HDMR com-  
 426 ponent functions are re-derived in the proposed PBQO method, along with some of the acquisition  
 427 functions;

428 c) The proposed PBQO method is able to support parallel distributed processing owing to the proposed  
 429 multi-point selection strategy, while both NIPI and CABO cannot. This advantage is desired when  
 430 each evaluation of the  $\mathcal{G}$ -function is costly and parallel computing facilities are available;



431 d) The proposed PBQO method is capable of yielding the REF, its variable importance and bounds  
 432 simultaneously with a single run. However, the NIPI method and CABO method are only designed  
 433 for evaluating the variable importance and bounds, respectively.

#### 434 4. Extending the proposed method to Case IV

435 The proposed PBQO method is mainly illustrated in case that hybrid uncertainties present as both  
 436 random variables and interval variables. When parameterized p-boxes are involved, the proposed method  
 437 is also applicable, but needs slight adaptations. In this section, we will show how to extend the proposed  
 438 PBQO method established in Section 3 to **Case IV**.

439 Let  $\mathbf{Y} = [Y_1, Y_2, \dots, Y_{d_3}]$  denote an imprecise random vector containing  $d_3$  variables. These variables  
 440 are assumed to be characterized by parameterized p-boxes, and their joint PDF is denoted as  $f_{\mathbf{Y}|\boldsymbol{\theta}}(\mathbf{y}|\boldsymbol{\theta})$ ,  
 441 which depends on a set of  $d_4$  interval variables  $\boldsymbol{\Theta} = [\Theta_1, \Theta_2, \dots, \Theta_{d_4}]$  with lower and upper bounds  $\underline{\boldsymbol{\theta}} =$   
 442  $[\underline{\theta}_1, \underline{\theta}_2, \dots, \underline{\theta}_{d_4}]$  and  $\bar{\boldsymbol{\theta}} = [\bar{\theta}_1, \bar{\theta}_2, \dots, \bar{\theta}_{d_4}]$ , respectively. In **Case IV**, the response function is represented by  
 443  $Z = g(\mathbf{X}, \mathbf{Y}, \mathbf{A})$ . In analogy to **Case III**, an augmented response function  $Z = g(\mathbf{X}, \mathbf{Y}, \mathbf{A}, \boldsymbol{\Theta})$  needs to be  
 444 artificially constructed to account for  $\boldsymbol{\Theta}$  like  $\mathbf{A}$ . Then, we map the random vector  $\{\mathbf{X}, \mathbf{Y}\}$  to a standard  
 445 normal one  $\mathbf{U}$ , while the interval vector  $\{\mathbf{A}, \boldsymbol{\Theta}\}$  to a standard interval one  $\mathbf{V}$ . Accordingly, the response  
 446 function is changed to be  $Z = \mathcal{G}(\mathbf{W})$ , where  $\mathbf{W} = \{\mathbf{U}, \mathbf{V}\}$ . See, e.g., [39–41], for the details of how to use  
 447 an augmented response function when parameterized p-boxes are involved. Note that this does not mean  
 448 that the original  $g$ -function has to be modified, but only for numerical implementation. By doing so, the  
 449 remaining procedures are similar to those given in Section 3.

#### 450 5. Numerical examples

451 In this section, three numerical examples are investigated to demonstrate the proposed method. For  
 452 comparison purposes, the NIPI and CABO methods are mainly implemented in all examples. These methods  
 453 are used in a similar way as the proposed PBQO method since they are originally developed for only  
 454 propagating parameterized p-boxes. Besides, in both methods the support of interval variables has been  
 455 increased by 10% and the stopping tolerances are specified in accordance with the proposed method.

##### 456 5.1. Example 1: A test function

457 Consider a test function of the form:

$$Z = g(X, A_1, A_2) = X^2 + A_1 + A_2^3, \quad (34)$$

458 where  $X$ ,  $A_1$  and  $A_2$  are three uncertain input variables, as listed in Tab. 1.

Table 1: Uncertainty characterization of input variables for Example 1.

Notation	Type	Mathematical model
$X$	Random variable	$\mathcal{N}(0, 1^2)$
$A_1$	Interval variable	[1 2]
$A_2$	Interval variable	[1 2]

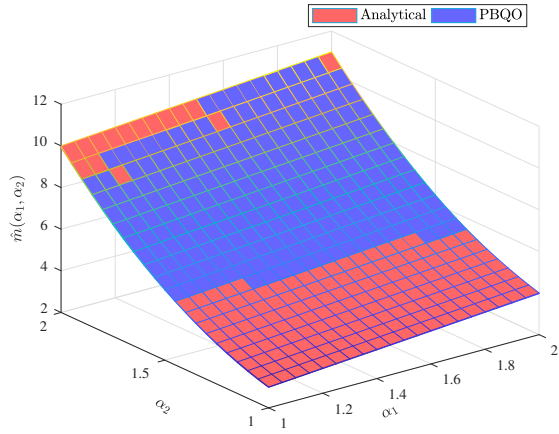
Note:  $\mathcal{N}$  stands for normal distribution.

459 We first consider the REF  $m(\alpha_1, \alpha_2)$ , the closed-form expression of which is obtained as  $m(\alpha_1, \alpha_2) =$   
460  $1 + \alpha_1 + \alpha_2^3$ . The proposed PBQO method can be implemented to yield a numerical estimate of  $m(\alpha_1, \alpha_2)$ .  
461 In this example, we set  $c = 2$ ,  $n_0 = 5$ ,  $\varepsilon^{\text{BPI}} = 0.02$  and  $\varepsilon^{\text{BGO}} = 0.002$ . Fig. 2(a) depicts the REF estimated  
462 by PBQO v.s. its analytical solution, which coincide almost perfectly. Besides, as shown in Fig. 2(b) the  
463 coefficient of variation (COV) of the PBQO estimate is quite small, indicating that the estimate is highly  
464 reliable. In order to compare with other existing methods, we also employ the NIPI and CABO methods  
465 in this example. It can be seen from Figs. 2(c) and 2(e) that both NIPI and CABO methods give poor  
466 estimates for the ERF, especially in the boundary area. In addition, Figs. 2(d) and 2(f) show that the  
467 results by these two methods also **process** relatively large variability.

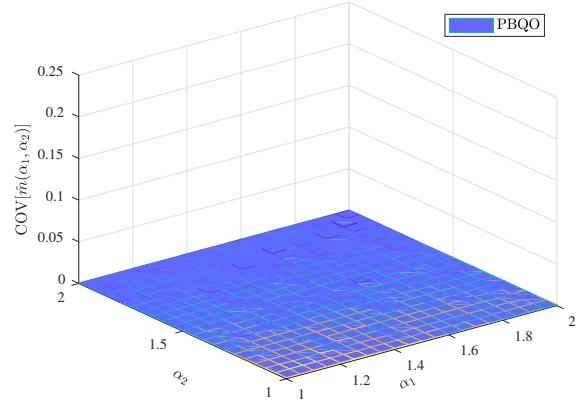
468 Second, the RS-HDMR component functions of the REF are of concern. For limiting the paper length,  
469 we just show the first-order RS-HDMR component functions as an illustration. The analytical expressions  
470 of  $m_1(\alpha_1)$  and  $m_2(\alpha_2)$  can be derived as:  $m_1(\alpha_1) = -\frac{3}{2} + \alpha_1$  and  $m_2(\alpha_2) = -\frac{15}{4} + \alpha_2^3$ . From Fig. 3, one  
471 can observe that for both component functions: (1) the proposed PBQO method is able to yield very close  
472 estimates to analytical solutions; (2) the 99% confidence intervals (CIs) of PBQO estimates are very narrow;  
473 (3) the NIPI and CABO methods are shown to be less accurate than the proposed method; (4) the 99%  
474 CIs of both NIPI and CABO estimates are obviously wider than these by the proposed method. These  
475 observations demonstrate the accuracy of the proposed method against both NIPI and CABO methods.  
476 Besides, through the first-order RS-HDMR component functions it is easy to know that  $\alpha_2$  has significantly  
477 larger influence on the REF than  $\alpha_1$ . Therefore, if one would like to reduce the epistemic uncertainty in the  
478 REF (i.e., narrow the interval), a more rational way is to shrink  $A_2$  by collecting more data of it.

479 Third, we discuss the results of the response expectation bounds. The analytical lower and upper bounds  
480 of the REF are 3 and 11, respectively. Tab. 2 compares the numerical estimates given by the PBQO, NIPI  
481 and CABO methods to the analytical solutions. It can be seen that for both lower and upper bounds:  
482 (1) PBQO and CABO methods are capable of producing close estimates to the analytical solutions, and  
483 restively small posterior COVs; (2) NIPI method gives poor estimates with large posterior COV.

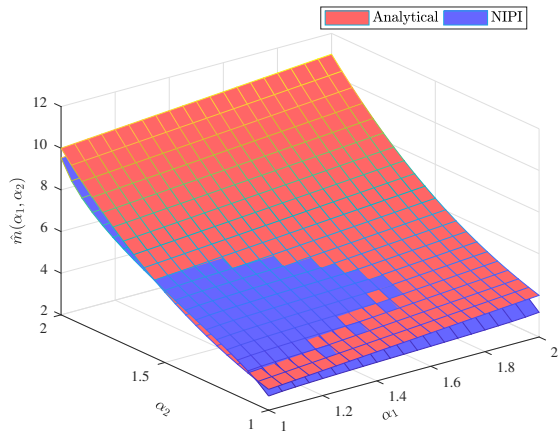
484 At last, the efficiency and accuracy of these three methods should be emphasized. As listed in Tab. 2,  
485 the number of response function evaluations for the PBQO, NIPI and CABO is 13, 8 and 22, respectively.



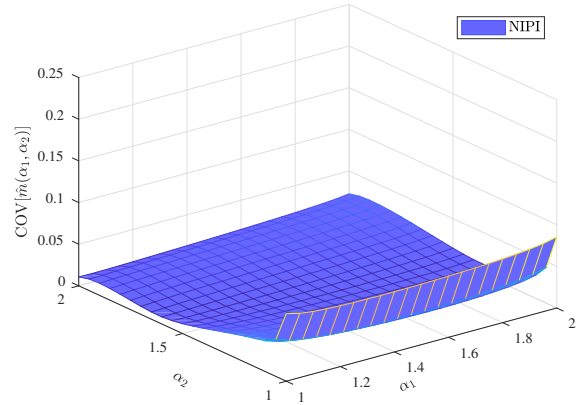
(a)



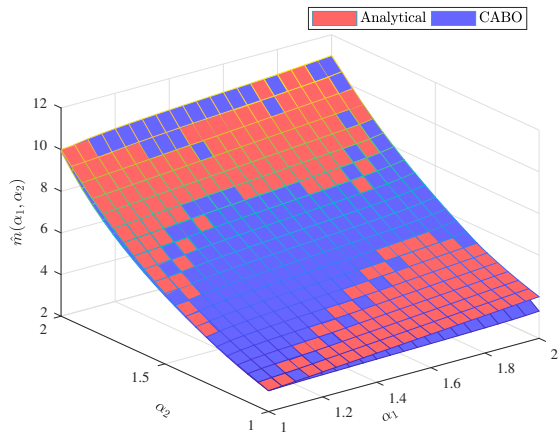
(b)



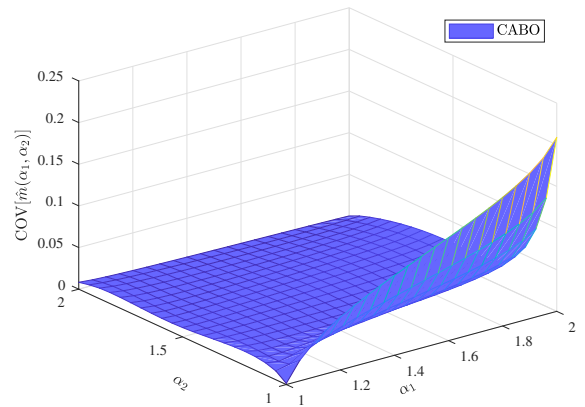
(c)



(d)



(e)



(f)

Figure 2: Response expectation function for Example 1 by different methods.

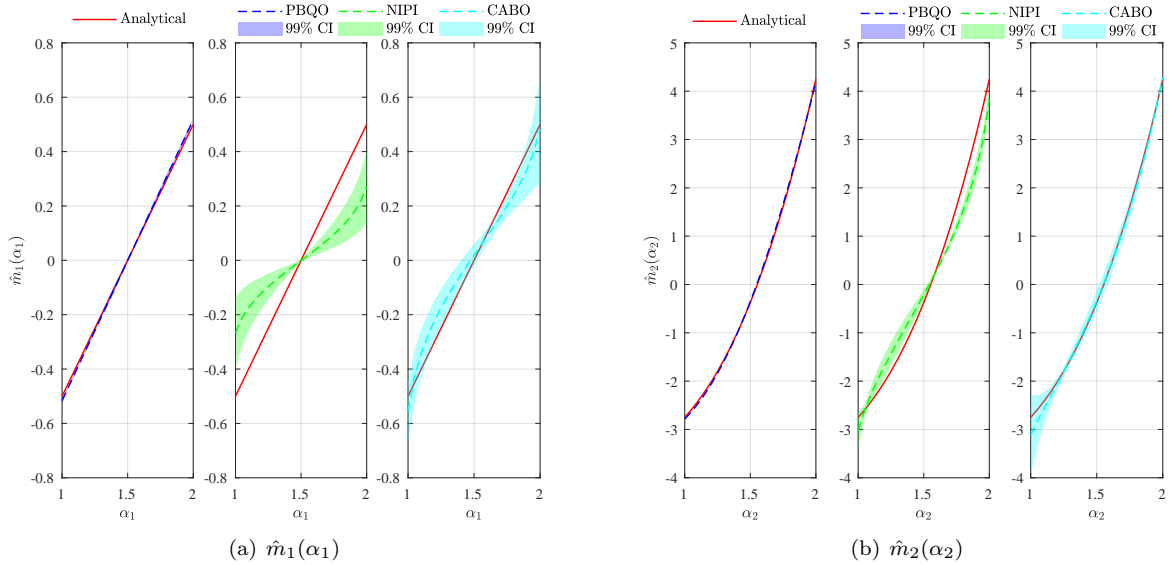


Figure 3: First-order RS-HDMR component functions for Example 1 by different methods.

486 However, the PBQO method can support for parallel computing, and hence its number of calls to the  
 487 response function for each CPU core is only 6.5 on average. To this end, the number of effective response  
 488 function evaluations required by the proposed PBQO method is close to that of the NIPI method, but  
 489 less than the CABO method. Besides, the proposed PBQO method is able to produce the REF, its RS-  
 490 HDMR component functions and bound simultaneously with reasonable accuracy, while the NIPI method  
 491 may perform worse in all these three aspects and the CABO method could be reliable only in capturing the  
 492 REF bounds.

Table 2: Response expectation bound for Example 1.

Method	$\hat{m}_l$	COV $[\hat{m}_l]$ /%	$\hat{m}_u$	COV $[\hat{m}_u]$ /%	$N$	$\frac{N}{c}$
Analytical	3	-	11	-	-	-
PBQO ( $c = 2$ )	2.9820	0.22	11.0027	0.00	5+8=13	6.5
NIPI ( $c = 1$ )	2.6795	8.11	10.0148	2.26	5+3=8	8
CABO ( $c = 1$ )	3.0033	0.08	10.9966	0.00	5+17=22	22

Note:  $N$  is the total number of response function evaluations;  $c$  is the number of points selected at each iteration, and hence the number of CPU cores used in parallel; and  $N/c$  is referred to as the number of effective response function evaluations.

493 5.2. Example 2: A non-linear oscillator

494 The second example considers a nonlinear undamped single degree-of-freedom (SDOF) oscillator sub-  
 495 jected to a rectangular pulse load (as shown in Fig. 4), which was extensively studied in context of reliability  
 496 analysis (see, e.g., [39, 61, 62]). The response function is defined as the maximum displacement of the oscil-  
 497 lator:

$$Z = g(c_1, c_2, m, F_1, t_1) = \left| \frac{2F_1}{c_1 + c_2} \sin \left( \frac{t_1}{2} \sqrt{\frac{c_1 + c_2}{m}} \right) \right|, \quad (35)$$

498 where  $c_1, c_2, m, F_1, t_1$  are five uncertain input variables, detailed description of which can be found in Tab.  
 499 3. For notational clarity, we denote the three intervals as  $A_1 = [1 \ 2]$ ,  $A_2 = [0.1 \ 0.3]$  and  $A_3 = [0.5 \ 1.5]$  in  
 500 what follows.

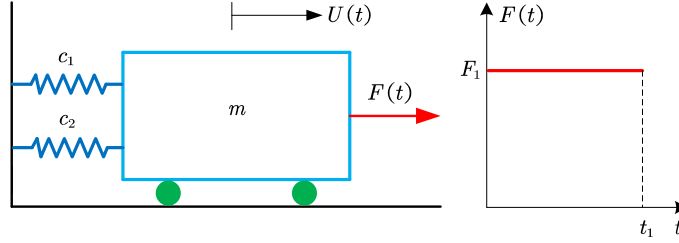


Figure 4: A nonlinear SDOF oscillator subjected to a rectangular pulse load.

Table 3: Uncertainty characterization of input variables for Example 2.

Notation	Type	Mathematical model
$c_1$	Random variable	$\mathcal{N}(1, 0.1^2)$
$c_2$	Random variable	$\mathcal{N}(0.1, 0.01^2)$
$m$	Random variable	$\mathcal{N}(1, 0.1^2)$
$F_1$	P-box variable	$\mathcal{LN}([1 \ 2], [0.1 \ 0.3]^2)$
$t_1$	Interval variable	$[0.5 \ 1.5]$

Note:  $\mathcal{LN}$  stands for Lognormal distribution.

501 In this example, the REF, its RS-HDMR component functions and bounds are also of our interest. Due  
 502 to the complexity of the response function, the corresponding analytical solutions are not available, and  
 503 thus we use Monte Carlo simulation (MCS) or double-loop MCS (DL-MCS) [63] to provide reference results.  
 504 The initial parameters of the proposed PBQO method are specified as:  $c = 4$ ,  $n_0 = 15$ ,  $\varepsilon^{\text{BPI}} = 0.01$  and  
 505  $\varepsilon^{\text{BGO}} = 0.001$ . It should be noted that the REF is three-dimensional, and hence we simply set  $\alpha_3 = 1$  in  
 506 order to visualize the results. As can be seen from Fig. 5(b), the COV of the MCS estimate is extremely  
 507 small, indicating that we can take the MCS estimate as a reference result. From Figs. 5(a), 5(c) and 5(e),  
 508 it is obvious that the proposed PBQO method can produce a much better REF estimate than the NIPI

509 and CABO methods. Besides, the posterior COV of the PBQO estimate is also much smaller than those  
510 by NIPI and CABO methods, as shown in Figs. 5(b), 5(d) and 5(f). As for the RS-HDMR component  
511 functions of the REF, we only give three first-order RS-HDMR component functions  $\hat{m}_1(\alpha_1)$ ,  $\hat{m}_2(\alpha_2)$  and  
512  $\hat{m}_3(\alpha_3)$  as an illustration. It can be seen from Fig. 6 that for all the three component functions the proposed  
513 PBQO method can produce fairly good results, in comparison to these given by MCS. However, the NIPI  
514 and CABO methods perform much worse than PBQO, especially for  $\hat{m}_2(\alpha_2)$ . Tab. 4 compares the lower  
515 and upper bounds of the REF by different methods. As can be seen, the PBQO and CABO methods are  
516 able to yield desirable estimates with relatively small posterior COVs, while the NIPI method does not work  
517 well. It should be noted that the proposed method only requires 7.75 effective response function evaluations  
518 to produce the above results, which are less than those by NIPI and CABO.

Table 4: Response expectation bound for Example 2.

Method	$\hat{m}_l$	COV $[\hat{m}_l]$ /%	$\hat{m}_u$	COV $[\hat{m}_u]$ /%	$N$	$\frac{N}{c}$
DL-MCS	0.4953	0.87	2.5766	0.37	$10^6$	-
PBQO ( $c = 4$ )	0.4583	0.35	2.5935	0.07	15+16=31	7.75
NIPI ( $c = 1$ )	0.4160	15.94	2.6343	3.04	15+3=18	18
CABO ( $c = 1$ )	0.4721	0.25	2.5866	0.08	15+24=39	38

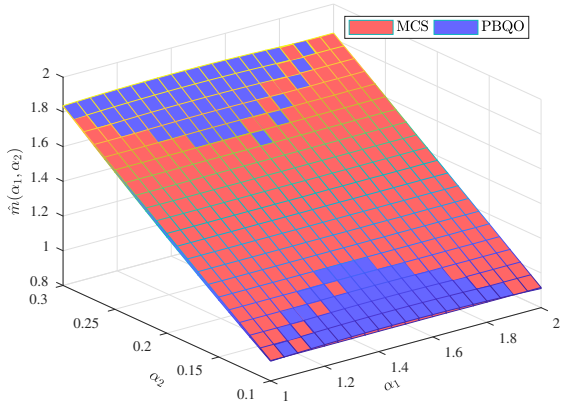
### 519 5.3. Example 3: A 56-bar spatial truss structure

520 The third example consists of a 56-bar spatial truss structure, as shown in Fig. 7. Nine vertical loads  
521 are applied to the structure at joints 1-9, which are denoted as  $P_1 \sim P_9$ . The external loads  $P_1 - P_9$  are  
522 assumed to be uncertain, together with the elastic modulus  $E$  and cross-sectional area  $A$ . These uncertainties  
523 are characterized by three kinds of models, which are summarized in Tab. 5. It can be seen that four  
524 intervals are involved and we denote them as  $A_1 = [20 \ 30]$  kN,  $A_2 = [30 \ 40]$  kN,  $A_3 = [200 \ 220]$  Gpa and  
525  $A_4 = [150 \ 250]$  mm<sup>2</sup>. The response of concern is selected as the vertical displacement of joint 1, which can  
526 implicitly expressed as a function of  $P_1 \sim P_9$ ,  $E$  and  $A$ , i.e.,  $Z = g(P_1 \sim P_9, E, A)$ .

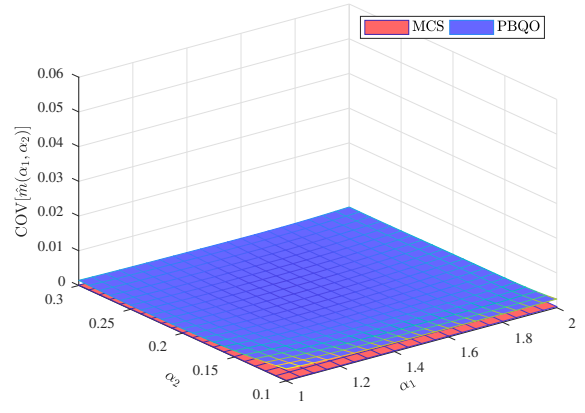
Table 5: Uncertainty characterization of input variables for Example 3.

Notation	Type	Unit	Mathematical model
$P_2 \sim P_9$	Random variable	kN	$\mathcal{LN}(20, 4^2)$
$P_1$	P-box variable	kN	$\mathcal{LN}([20 \ 30], [30 \ 40]^2)$
$E$	Interval variable	GPa	[200 220]
$A$	Interval variable	mm <sup>2</sup>	[150 250]

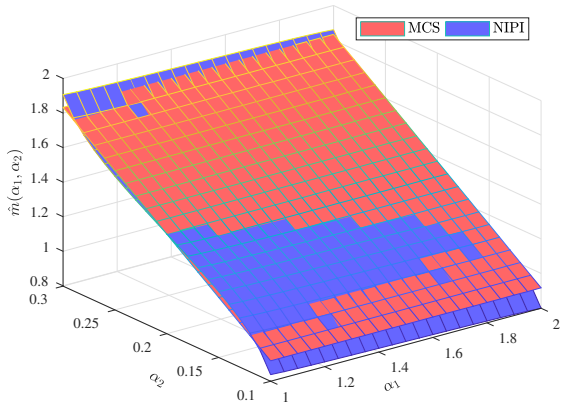
527 The proposed PBQO method is initialized with  $c = 4$ ,  $n_0 = 20$ ,  $\varepsilon^{\text{BPI}} = 0.02$  and  $\varepsilon^{\text{BGO}} = 0.002$ . Fig. 8  
528 depicts the REF estimates by three methods and their corresponding posterior COVs, where we fix  $\alpha_3$  and



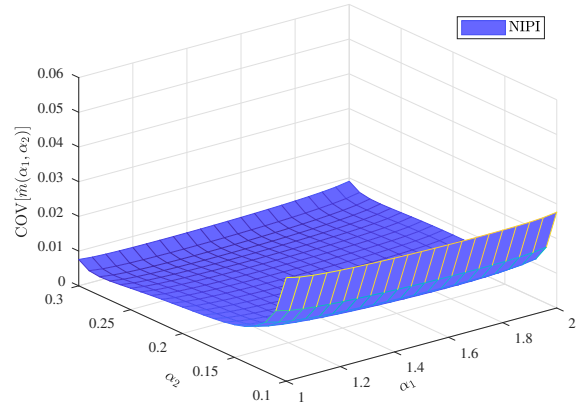
(a)



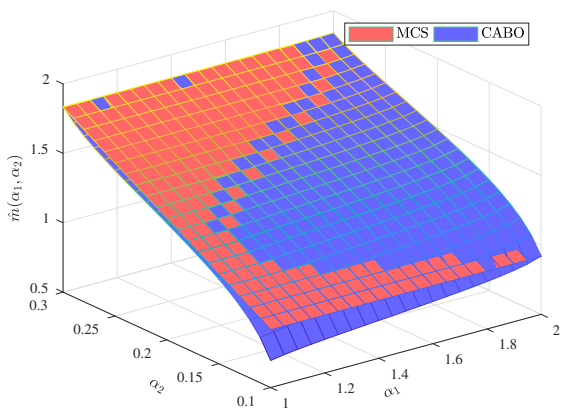
(b)



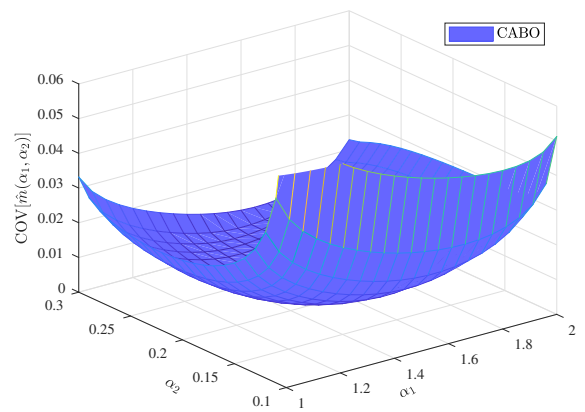
(c)



(d)



(e)



(f)

Figure 5: Response expectation function for Example 2 by different methods ( $\alpha_3 = 1$ ).

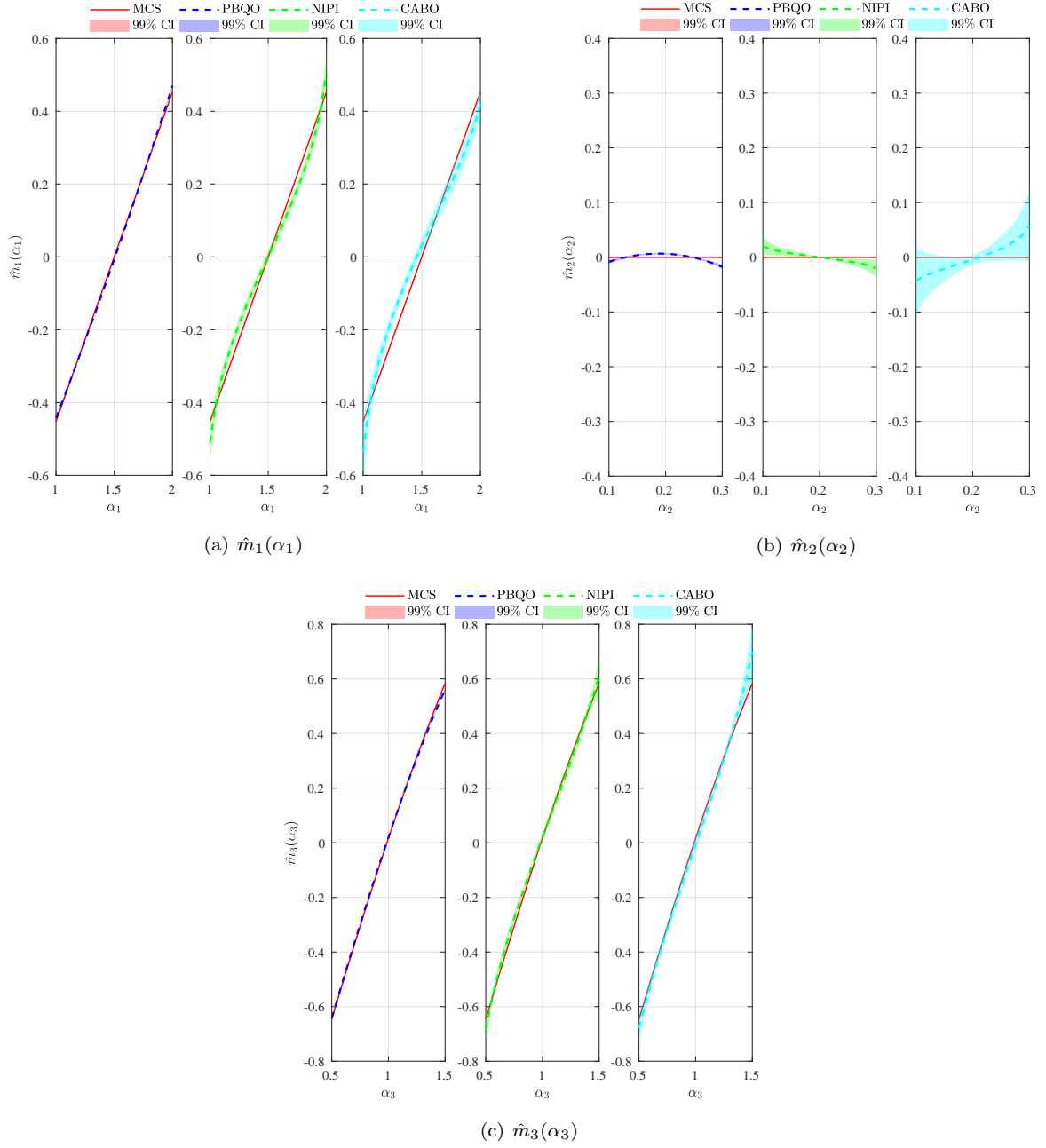


Figure 6: First-order RS-HDMR component functions for Example 2 by different methods.

529  $\alpha_4$  at their midpoints, i.e.,  $\alpha_3 = 210$  Gpa and  $\alpha_4 = 200$  mm<sup>2</sup>. It is shown that the posterior COV of the  
530 PBQO estimate is much smaller than those by both NIPI and CABO methods, indicating that the proposed  
531 PBQO method is more reliable for capturing the REF. The results of four first-order HDMR component  
532 functions in Fig. 9 also imply that the proposed method has better accuracy than the NIPI and CABO  
533 methods. Besides, it is easy to know from Fig. 9 that the four intervals can be ranked as  $A_4 > A_1 > A_3 > A_2$



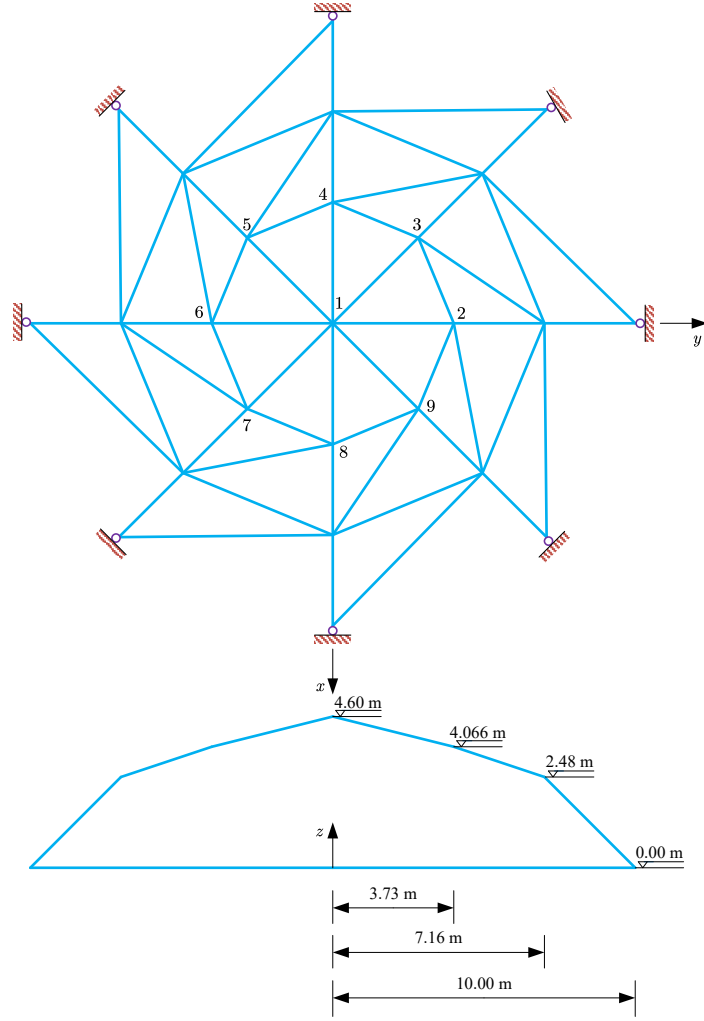
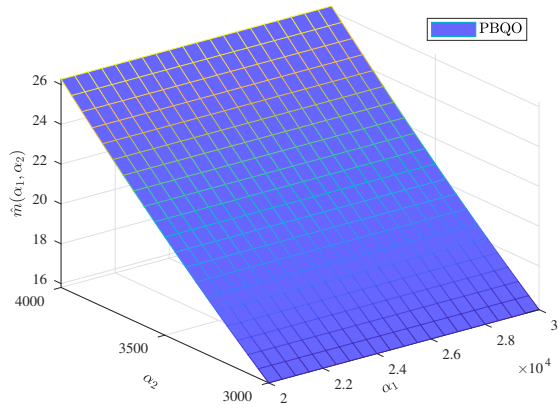


Figure 7: A 56-bar spatial truss structure.

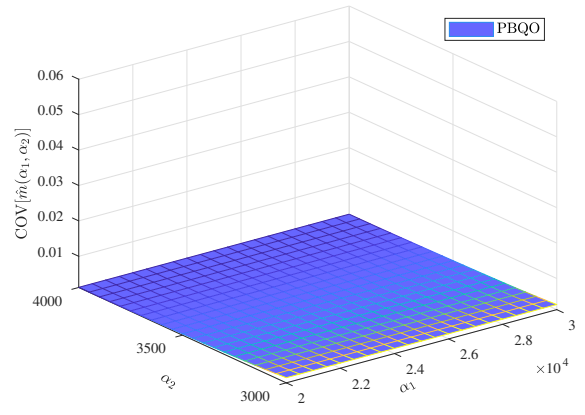
534 in terms of their first-order importance to the REF. Through Tab. 6, one can find that for both lower and  
 535 upper bounds of the REF the PBQO and CABO can yield better estimates than the NIPI, indicating by  
 536 their posterior COVs. It should be emphasized that by taking advantage of parallel computing the effective  
 537 response function calls required by the proposed PBQO method are much less than that of CABO.

Table 6: Response expectation bound for Example 3.

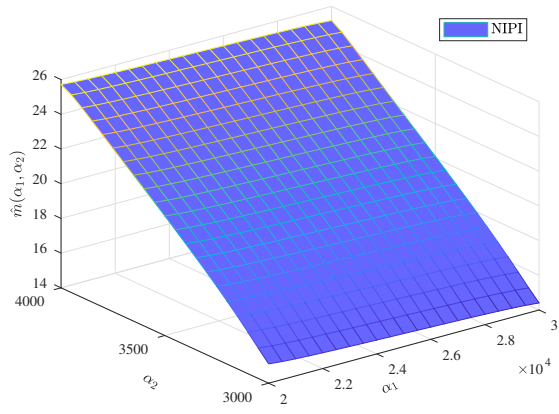
Method	$\hat{m}_l$	COV $[\hat{m}_l]$ /%	$\hat{m}_u$	COV $[\hat{m}_u]$ /%	$N$	$\frac{N}{c}$
DL-MCS	11.1793	2.11	35.2535	1.64	$10^4$	-
PBQO ( $c = 4$ )	11.8785	0.23	35.4109	0.08	20+12=32	8
NIPI ( $c = 1$ )	12.5791	4.74	34.4007	2.36	20+2=22	22
CABO ( $c = 1$ )	11.5818	0.12	35.3302	0.07	20+23=43	43



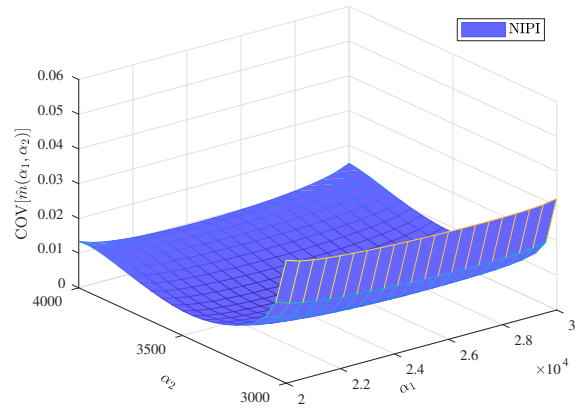
(a)



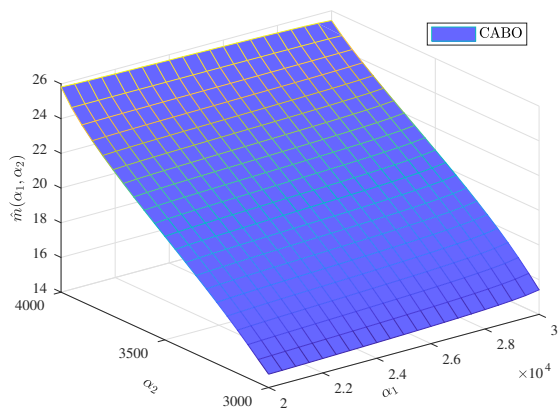
(b)



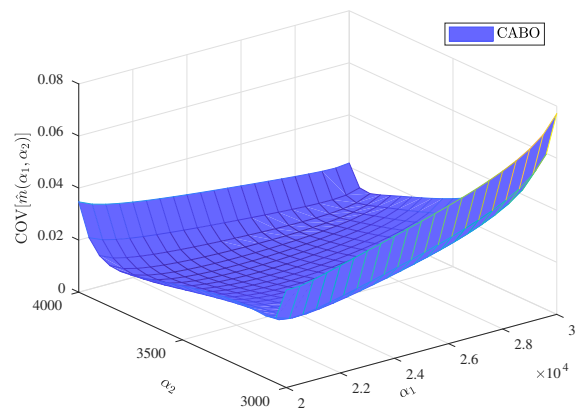
(c)



(d)



(e)



(f)

Figure 8: Response expectation function for Example 3 by different methods ( $\alpha_3 = 210$  Gpa and  $\alpha_4 = 200$  mm<sup>2</sup>).

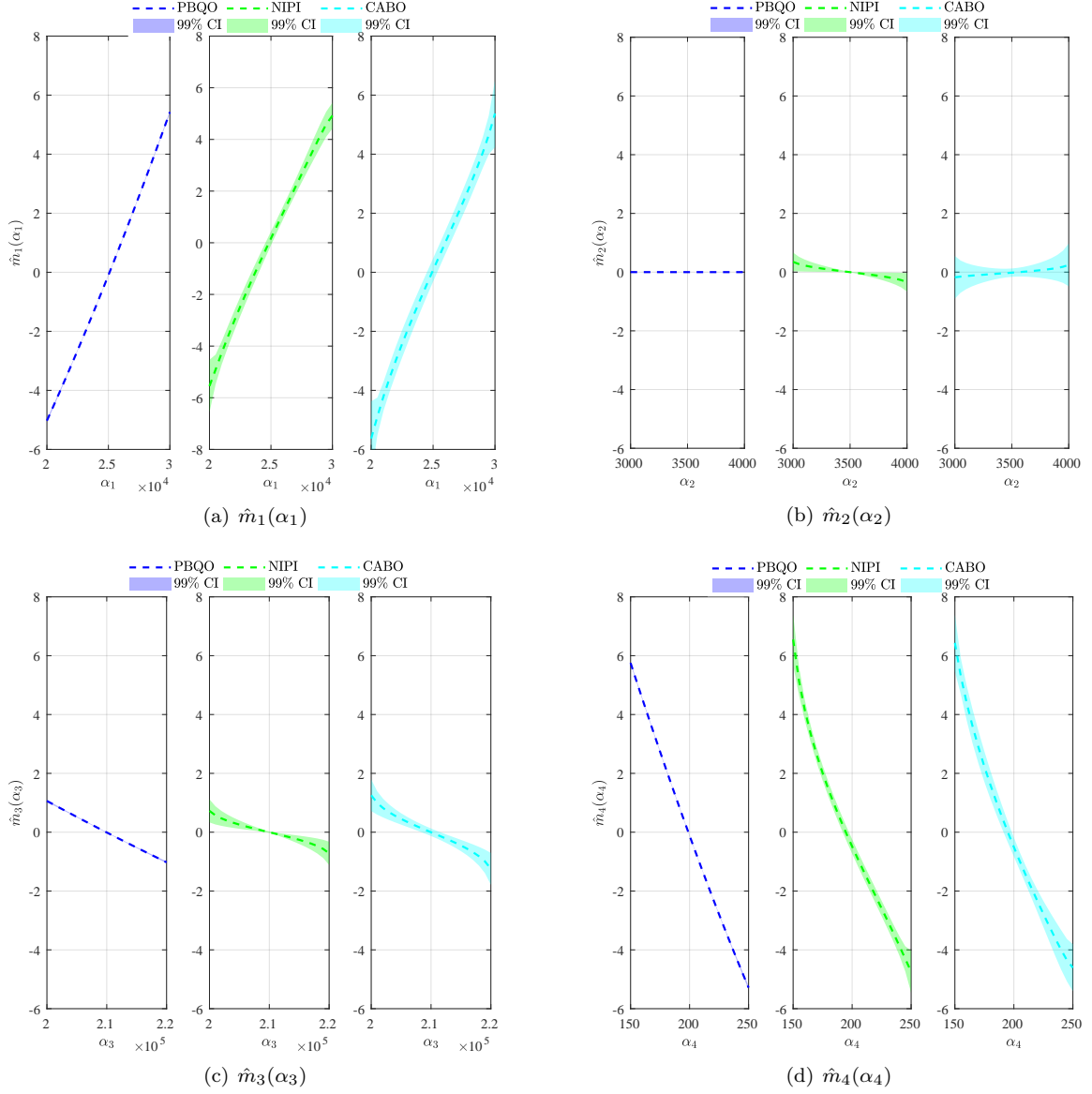


Figure 9: First-order RS-HDMR component functions for Example 3 by different methods.

## 538 6. Conclusions and perspectives

539 In this work, propagation of hybrid uncertainties in the form of precise random variables, parameterized  
540 p-boxes and interval variables is studied via Bayesian numerical analysis. The main contribution lies in  
541 the development of a novel method, termed ‘Parallel Bayesian Quadrature Optimization’, for estimation of  
542 response expectation function, its RS-HDMR component functions and bounds simultaneously. Compared  
543 to the state-of-the-art methods for propagating hybrid uncertainties, the proposed method has several sig-  
544 nificant advantages. First, the proposed method breaks the double-loop paradigm that typically propagates

545 aleatory and epistemic uncertainty separately in a nested way. That is, it can propagate both types of  
 546 uncertainties simultaneously, and is a fully-decoupled procedure in nature, yielding a major improvement  
 547 in computational efficiency. Second, the proposed method is able to exploit prior knowledge thanks to its  
 548 Bayesian nature, and it also supports parallel computing, further leading to much higher computational  
 549 efficiency. Third, the estimators (i.e., posterior means) of the response moment function and its RS-HDMR  
 550 component functions are analytically derived, together with their posterior variances for indicating numerical  
 551 errors.

552 While these advantages are encouraging, there are still some issues that need further study. For example,  
 553 one should note that the analytical tractability of the proposed method is based on using the squared  
 554 exponential kernel that is appropriate for modelling smooth and moderately nonlinear functions. This,  
 555 however, is not always justified for a general practical problem. Besides, the proposed method relies on a  
 556 total number of five acquisition functions, which could be reduced by developing more efficient Bayesian  
 557 experimental design strategies. **The proposed method could be extended to evaluate the second-order raw**  
 558 **moment function, while more research efforts may still be required.**

#### 559 Declaration of competing interest

560 The authors declare that they have no known competing financial interests or personal relationships that  
 561 could have appeared to influence the work reported in this paper.

#### 562 Acknowledgments

563 Chao Dang is mainly supported by China Scholarship Council (CSC). Pengfei Wei is grateful to the  
 564 support from the National Natural Science Foundation of China (grant no. 51905430 and and 72171194).  
 565 Chao Dang, Pengfei Wei and Michael Beer also would like to appreciate the support of Sino-German Mobility  
 566 Program under grant number M-0175.

#### 567 Appendix A. Derivation of the posterior variance for the first-order RS-HDMR component 568 function

569 The posterior variance function  $\sigma_{\hat{\mathcal{M}}_i}^2(v_i)$  for the first-order RS-HDMR function  $\hat{\mathcal{M}}_i(v_i)$  can be given by:

$$\sigma_{\hat{\mathcal{M}}_i}^2(v_i) = \mathbb{V}_{\mathcal{D}} \left[ \hat{\mathcal{M}}_i(v_i) \right] = \mathbb{V}_{\mathcal{D}} \left[ \Pi_{-v_i} [\mathcal{G}(\mathbf{w})] \right] + \sigma_{\hat{\mathcal{M}}_0}^2 - 2\text{COV}_{\mathcal{D}} \left[ \Pi_{-v_i} [\hat{\mathcal{G}}(\mathbf{w})], \hat{\mathcal{M}}_0 \right], \quad (\text{A.1})$$

570 where  $\text{COV}_{\mathcal{D}}[\cdot, \cdot]$  refers to the covariance taken with respect to the posterior distributions of its arguments  
 571 given data  $\mathcal{D}$ ; the term  $\sigma_{\hat{\mathcal{M}}_0}^2$  has been given in Eq. (17).

572 The term  $\mathbb{V}_{\mathcal{D}} [\Pi_{-v_i} [\mathcal{G}(\mathbf{w})]]$  in Eq. (A.1) can be further deduced by applying Fubini's theorem such that:

$$\mathbb{V}_{\mathcal{D}} [\Pi_{-v_i} [\mathcal{G}(\mathbf{w})]] = \Pi_{-v_i} \Pi_{-v_i} \left[ k_0 \left( \mathbf{w}, \left( \mathbf{w}'_{-v'_i}, v_i \right) \right) \right] - \Pi_{-v_i} \left[ \mathbf{k}_0(\mathbf{w}, \mathcal{W})^T \right] \mathbf{K}_0^{-1} \Pi_{-v_i} \left[ \mathbf{k}_0(\mathbf{w}, \mathcal{W}) \right], \quad (\text{A.2})$$

573 where the term  $\Pi_{-v_i} \left[ \mathbf{k}_0(\mathbf{w}, \mathcal{W}) \right]$  has been given in Eq. (21); the term  $\Pi_{-v_i} \Pi_{-v_i} \left[ k_0 \left( \mathbf{w}, \left( \mathbf{w}'_{-(d_1+i)}, v_i \right) \right) \right]$   
574 can be derived as:

$$\begin{aligned} & \Pi_{-v_i} \Pi_{-v_i} \left[ k_0 \left( \mathbf{w}, \left( \mathbf{w}'_{-(d_1+i)}, v_i \right) \right) \right] \\ &= s_0^2 \left| 2\boldsymbol{\Sigma}_{\mathbf{u}}^{-1} + \mathbf{I} \right|^{-1/2} \\ & \cdot 2^{(d_2-1)} \text{prod}_1 \left\{ \text{diag} \left\{ \boldsymbol{\Sigma}_{\mathbf{v}_{-i}} \left[ -1 + \exp \left[ -(2\boldsymbol{\Sigma}_{\mathbf{v}_{-i}})^{-1} \right] + (2\pi^{-1} \boldsymbol{\Sigma}_{\mathbf{v}_{-i}})^{-1/2} \text{erf} \left( (2\boldsymbol{\Sigma}_{\mathbf{v}_{-i}})^{-1/2} \right) \right] \right\} \right\}. \end{aligned} \quad (\text{A.3})$$

575 Likewise, the term  $\text{COV}_{\mathcal{D}} \left[ \Pi_{-v_i} \left[ \hat{\mathcal{G}}(\mathbf{w}) \right], \hat{\mathcal{M}}_0 \right]$  in Eq. (A.1) can be formulated as:

$$\text{COV}_{\mathcal{D}} \left[ \Pi_{-v_i} \left[ \hat{\mathcal{G}}(\mathbf{w}) \right], \hat{\mathcal{M}}_0 \right] = \Pi_{-v_i} \Pi \left[ k_0(\mathbf{w}, \mathbf{w}') \right] - \Pi_{-v_i} \left[ \mathbf{k}_0(\mathbf{w}, \mathcal{W})^T \right] \mathbf{K}_0^{-1} \Pi \left[ \mathbf{k}_0(\mathbf{w}, \mathcal{W}) \right], \quad (\text{A.4})$$

576 where

$$\begin{aligned} & \Pi_{-v_i} \Pi \left[ k_0(\mathbf{w}, \mathbf{w}') \right] \\ &= s_0^2 \left| 2\boldsymbol{\Sigma}_{\mathbf{u}}^{-1} + \mathbf{I} \right|^{-1/2} \\ & \cdot 2^{(d_2-1)} \text{prod}_1 \left\{ \text{diag} \left\{ \boldsymbol{\Sigma}_{\mathbf{v}_{-i}} \left[ -1 + \exp \left[ -(2\boldsymbol{\Sigma}_{\mathbf{v}_{-i}})^{-1} \right] + (2\pi^{-1} \boldsymbol{\Sigma}_{\mathbf{v}_{-i}})^{-1/2} \text{erf} \left( (2\boldsymbol{\Sigma}_{\mathbf{v}_{-i}})^{-1/2} \right) \right] \right\} \right\} \\ & \cdot \left( \frac{\pi}{2} \right)^{1/2} \text{prod}_2 \left\{ \left[ \text{erf} \left( (1 - v_i) (2\boldsymbol{\Sigma}_{\mathbf{v}_i})^{-1/2} \right) - \text{erf} \left( -v_i (2\boldsymbol{\Sigma}_{\mathbf{v}_i})^{-1/2} \right) \right] \boldsymbol{\Sigma}_{\mathbf{v}_i}^{1/2} \right\}. \end{aligned} \quad (\text{A.5})$$

## 577 Appendix B. Derivation of the posterior variance for the second-order RS-HDMMR component 578 function

579 The posterior variance function  $\sigma_{\hat{\mathcal{M}}_{ij}}^2(v_i, v_j)$  for the second-order RS-HDMMR component function  $\hat{\mathcal{M}}_{ij}(v_i, v_j)$   
580 can be formulated as:

$$\begin{aligned} \sigma_{\hat{\mathcal{M}}_{ij}}^2(v_i, v_j) &= \mathbb{V}_{\mathcal{D}} \left[ \hat{\mathcal{M}}_{ij}(v_i, v_j) \right] \\ &= \mathbb{V}_{\mathcal{D}} \left[ \Pi_{-v_{ij}} [\mathcal{G}(\mathbf{w})] \right] + \sigma_{\hat{\mathcal{M}}_i}^2(v_i) + \sigma_{\hat{\mathcal{M}}_j}^2(v_j) + \sigma_{\hat{\mathcal{M}}_0}^2 \\ & \quad - 2\text{COV}_{\mathcal{D}} \left[ \Pi_{-v_{ij}} [\mathcal{G}(\mathbf{w})], \Pi_{-v_i} [\mathcal{G}(\mathbf{w})] \right] - 2\text{COV}_{\mathcal{D}} \left[ \Pi_{-v_{ij}} [\mathcal{G}(\mathbf{w})], \Pi_{-v_j} [\mathcal{G}(\mathbf{w})] \right] \\ & \quad + 2\text{COV}_{\mathcal{D}} \left[ \Pi_{-v_{ij}} [\mathcal{G}(\mathbf{w})], \Pi [\mathcal{G}(\mathbf{w})] \right] + 2\text{COV}_{\mathcal{D}} \left[ \Pi_{-v_i} [\mathcal{G}(\mathbf{w})], \Pi_{-v_j} [\mathcal{G}(\mathbf{w})] \right] \\ & \quad - 2\text{COV}_{\mathcal{D}} \left[ \Pi_{-v_i} [\mathcal{G}(\mathbf{w})], \Pi [\mathcal{G}(\mathbf{w})] \right] - 2\text{COV}_{\mathcal{D}} \left[ \Pi_{-v_j} [\mathcal{G}(\mathbf{w})], \Pi [\mathcal{G}(\mathbf{w})] \right], \end{aligned} \quad (\text{B.1})$$

581 where the terms  $\sigma_{\hat{\mathcal{M}}_i}^2(v_i)$  and  $\sigma_{\hat{\mathcal{M}}_j}^2(v_j)$  can refer to Eq. (A.1); the term  $\sigma_{\hat{\mathcal{M}}_0}^2$  has been derived in Eq. (17);  
582 the last two covariance terms  $\text{COV}_{\mathcal{D}} \left[ \Pi_{-v_i} [\mathcal{G}(\mathbf{w})], \Pi [\mathcal{G}(\mathbf{w})] \right]$  and  $\text{COV}_{\mathcal{D}} \left[ \Pi_{-v_j} [\mathcal{G}(\mathbf{w})], \Pi [\mathcal{G}(\mathbf{w})] \right]$  has been  
583 given in Eq. (A.4).

584 The term  $\mathbb{V}_{\mathcal{D}} \left[ \Pi_{-v_{ij}} [\mathcal{G}(\mathbf{w})] \right]$  in Eq. (B.1) can be derived as:

$$\mathbb{V}_{\mathcal{D}} \left[ \Pi_{-v_{ij}} [\mathcal{G}(\mathbf{w})] \right] = \Pi_{-v_{ij}} \Pi_{-v_{ij}} \left[ k_0 \left( \mathbf{w}, \left( \mathbf{w}'_{-v'_{ij}}, v_{ij} \right) \right) \right] - \Pi_{-v_{ij}} \left[ \mathbf{k}_0(\mathbf{w}, \mathcal{W})^T \right] \mathbf{K}_0^{-1} \Pi_{-v_{ij}} \left[ \mathbf{k}_0(\mathbf{w}, \mathcal{W}) \right], \quad (\text{B.2})$$

585 where the term  $\Pi_{-\mathbf{v}_{ij}} [\mathbf{k}_0(\mathbf{w}, \mathcal{W})]$  has been given in Eq. (23); the term  $\Pi_{-\mathbf{v}_{ij}} \Pi_{-\mathbf{v}_{ij}} \left[ k_0 \left( \mathbf{w}, \left( \mathbf{w}'_{-\mathbf{v}'_{ij}}, \mathbf{v}_{ij} \right) \right) \right]$   
586 can be derived as:

$$\begin{aligned} & \Pi_{-\mathbf{v}_{ij}} \Pi_{-\mathbf{v}_{ij}} \left[ k_0 \left( \mathbf{w}, \left( \mathbf{w}'_{-\mathbf{v}'_{ij}}, \mathbf{v}_{ij} \right) \right) \right] \\ &= s_0^2 |2\boldsymbol{\Sigma}_{\mathbf{u}}^{-1} + \mathbf{I}|^{-1/2} \\ & \cdot 2^{(d_2-2)} \text{prod}_1 \left\{ \text{diag} \left\{ \boldsymbol{\Sigma}_{\mathbf{v}_{-ij}} \left[ -1 + \exp \left[ -(2\boldsymbol{\Sigma}_{\mathbf{v}_{-ij}})^{-1} \right] + (2\pi^{-1} \boldsymbol{\Sigma}_{\mathbf{v}_{-ij}})^{-1/2} \text{erf} \left( (2\boldsymbol{\Sigma}_{\mathbf{v}_{-ij}})^{-1/2} \right) \right] \right\} \right\}. \end{aligned} \quad (\text{B.3})$$

587 The term  $\text{COV}_{\mathcal{D}} [\Pi_{-\mathbf{v}_{ij}} [\mathcal{G}(\mathbf{w})], \Pi_{-v_i} [\mathcal{G}(\mathbf{w})]]$  in Eq. (B.1) is formulated as:

$$\text{COV}_{\mathcal{D}} [\Pi_{-\mathbf{v}_{ij}} [\mathcal{G}(\mathbf{w})], \Pi_{-v_i} [\mathcal{G}(\mathbf{w})]] = \Pi_{-\mathbf{v}_{ij}} \Pi_{-v_i} \left[ k_0 \left( \mathbf{w}, \left( \mathbf{w}'_{-v'_i}, v_i \right) \right) \right] - \Pi_{-\mathbf{v}_{ij}} \left[ \mathbf{k}_0(\mathbf{w}, \mathcal{W})^T \right] \mathbf{K}_0^{-1} \Pi_{-v_i} [\mathbf{k}_0(\mathbf{w}, \mathcal{W})], \quad (\text{B.4})$$

588 where the terms  $\Pi_{-\mathbf{v}_{ij}} [\mathbf{k}_0(\mathbf{w}, \mathcal{W})]$  and  $\Pi_{-v_i} [\mathbf{k}_0(\mathbf{w}, \mathcal{W})]$  have been given in Eq. (23) and Eq. (21) respec-  
589 tively; the term  $\Pi_{-\mathbf{v}_{ij}} \Pi_{-v_i} \left[ k_0 \left( \mathbf{w}, \left( \mathbf{w}'_{-v'_i}, v_i \right) \right) \right]$  can be derived as:

$$\begin{aligned} & \Pi_{-\mathbf{v}_{ij}} \Pi_{-v_i} \left[ k_0 \left( \mathbf{w}, \left( \mathbf{w}'_{-v'_i}, v_i \right) \right) \right] \\ &= s_0^2 |2\boldsymbol{\Sigma}_{\mathbf{u}}^{-1} + \mathbf{I}|^{-1/2} \\ & \cdot 2^{(d_2-2)} \text{prod}_1 \left\{ \text{diag} \left\{ \boldsymbol{\Sigma}_{\mathbf{v}_{-ij}} \left[ -1 + \exp \left[ -(2\boldsymbol{\Sigma}_{\mathbf{v}_{-ij}})^{-1} \right] + (2\pi^{-1} \boldsymbol{\Sigma}_{\mathbf{v}_{-ij}})^{-1/2} \text{erf} \left( (2\boldsymbol{\Sigma}_{\mathbf{v}_{-ij}})^{-1/2} \right) \right] \right\} \right\} \\ & \cdot \left( \frac{\pi}{2} \right)^{1/2} \text{prod}_2 \left\{ \left[ \text{erf} \left( (1 - v_j) (2\boldsymbol{\Sigma}_{\mathbf{v}_j})^{-1/2} \right) - \text{erf} \left( -v_j (2\boldsymbol{\Sigma}_{\mathbf{v}_j})^{-1/2} \right) \right] \boldsymbol{\Sigma}_{\mathbf{v}_j}^{1/2} \right\}. \end{aligned} \quad (\text{B.5})$$

590 Note that the term  $\text{COV}_{\mathcal{D}} [\Pi_{-\mathbf{v}_{ij}} [\mathcal{G}(\mathbf{w})], \Pi_{-v_j} [\mathcal{G}(\mathbf{w})]]$  in Eq. (B.1) can be similarly derived as the term  
591  $\Pi_{-\mathbf{v}_{ij}} \Pi_{-v_i} \left[ k_0 \left( \mathbf{w}, \left( \mathbf{w}'_{-(d_1+i)}, v_i \right) \right) \right]$  given in Eq. (B.4).

592 The covariance term  $\text{COV}_{\mathcal{D}} [\Pi_{-\mathbf{v}_{ij}} [\mathcal{G}(\mathbf{w})], \Pi [\mathcal{G}(\mathbf{w})]]$  in Eq. (B.1) can be formulated as:

$$\text{COV}_{\mathcal{D}} [\Pi_{-\mathbf{v}_{ij}} [\mathcal{G}(\mathbf{w})], \Pi [\mathcal{G}(\mathbf{w})]] = \Pi_{-\mathbf{v}_{ij}} \Pi [k_0(\mathbf{w}, \mathbf{w}')] - \Pi_{-\mathbf{v}_{ij}} \left[ \mathbf{k}_0(\mathbf{w}, \mathcal{W})^T \right] \mathbf{K}_0^{-1} \Pi [\mathbf{k}_0(\mathbf{w}, \mathcal{W})], \quad (\text{B.6})$$

593 where the terms  $\Pi [\mathbf{k}_0(\mathbf{w}, \mathcal{W})]$  and  $\Pi_{-\mathbf{v}_{ij}} [\mathbf{k}_0(\mathbf{w}, \mathcal{W})]$  have been given in Eq. (18) and Eq. 23 respectively;  
594 the term  $\Pi_{-\mathbf{v}_{ij}} \Pi [k_0(\mathbf{w}, \mathbf{w}')] can be derived as:$

$$\begin{aligned} & \Pi_{-\mathbf{v}_{ij}} \Pi [k_0(\mathbf{w}, \mathbf{w}')] \\ &= s_0^2 |2\boldsymbol{\Sigma}_{\mathbf{u}}^{-1} + \mathbf{I}|^{-1/2} \\ & \cdot 2^{(d_2-2)} \text{prod}_1 \left\{ \text{diag} \left\{ \boldsymbol{\Sigma}_{\mathbf{v}_{-ij}} \left[ -1 + \exp \left[ -(2\boldsymbol{\Sigma}_{\mathbf{v}_{-ij}})^{-1} \right] + (2\pi^{-1} \boldsymbol{\Sigma}_{\mathbf{v}_{-ij}})^{-1/2} \text{erf} \left( (2\boldsymbol{\Sigma}_{\mathbf{v}_{-ij}})^{-1/2} \right) \right] \right\} \right\} \\ & \cdot \left( \frac{\pi}{2} \right)^{2/2} \text{prod}_2 \left\{ \left[ \text{erf} \left( (1 - \mathbf{v}_{ij}) (2\boldsymbol{\Sigma}_{\mathbf{v}_{ij}})^{-1/2} \right) - \text{erf} \left( -\mathbf{v}_{ij} (2\boldsymbol{\Sigma}_{\mathbf{v}_{ij}})^{-1/2} \right) \right] \boldsymbol{\Sigma}_{\mathbf{v}_{ij}}^{1/2} \right\}. \end{aligned} \quad (\text{B.7})$$

595 The covariance term  $\text{COV}_{\mathcal{D}} [\Pi_{-v_i} [\mathcal{G}(\mathbf{w})], \Pi_{-v_j} [\mathcal{G}(\mathbf{w})]]$  in Eq. (B.1) can be formulated as:

$$\text{COV}_{\mathcal{D}} [\Pi_{-v_i} [\mathcal{G}(\mathbf{w})], \Pi_{-v_j} [\mathcal{G}(\mathbf{w})]] = \Pi_{-v_i} \Pi_{-v_j} \left[ k_0 \left( \mathbf{w}, \left( \mathbf{w}'_{-v'_j}, v_j \right) \right) \right] - \Pi_{-v_i} \left[ \mathbf{k}_0(\mathbf{w}, \mathcal{W})^T \right] \mathbf{K}_0^{-1} \Pi_{-v_j} [\mathbf{k}_0(\mathbf{w}, \mathcal{W})], \quad (\text{B.8})$$

596 where the terms  $\Pi_{-v_i} [k_0(\mathbf{w}, \mathcal{W})]$  and  $\Pi_{-v_j} [k_0(\mathbf{w}, \mathcal{W})]$  have been given in Eq. (21); the term  $\Pi_{-v_i} \Pi_{-v_j} [k_0(\mathbf{w}, (\mathbf{w}'_{-v'_j}, v_j))]$   
 597 is actually equal to  $\Pi_{-v_{ij}} \Pi [k_0(\mathbf{w}, \mathbf{w}')] as given in Eq. (B.7).$

## 598 References

- 599 [1] A. Der Kiureghian, O. Ditlevsen, Aleatory or epistemic? does it matter?, *Structural Safety* 31 (2) (2009) 105–112.
- 600 [2] M. Beer, S. Ferson, V. Kreinovich, Imprecise probabilities in engineering analyses, *Mechanical Systems and Signal Processing* 37 (1-2) (2013) 4–29.
- 601 [3] A. N. Kolmogorov, A. T. Bharucha-Reid, *Foundations of the theory of probability: Second English Edition*, Courier Dover Publications, 2018.
- 602 [4] D. Moens, D. Vandepitte, A survey of non-probabilistic uncertainty treatment in finite element analysis, *Computer Methods in Applied Mechanics and Engineering* 194 (12-16) (2005) 1527–1555.
- 603 [5] M. Faes, D. Moens, Recent trends in the modeling and quantification of non-probabilistic uncertainty, *Archives of Computational Methods in Engineering* 27 (3) (2020) 633–671.
- 604 [6] C. Jiang, R. Bi, G. Lu, X. Han, Structural reliability analysis using non-probabilistic convex model, *Computer Methods in Applied Mechanics and Engineering* 254 (2013) 83–98.
- 605 [7] T. Augustin, F. P. Coolen, G. De Cooman, M. C. Troffaes, *Introduction to imprecise probabilities*, John Wiley & Sons, 2014.
- 606 [8] S. Ferson, V. Kreinovich, L. Grinzburg, D. Myers, K. Sentz, *Constructing probability boxes and dempster-shafer structures*, Tech. rep., Sandia National Lab.(SNL-NM), Albuquerque, NM (United States) (2015).
- 607 [9] Z. Zhang, C. Jiang, Evidence-theory-based structural reliability analysis with epistemic uncertainty: a review, *Structural and Multidisciplinary Optimization* (2021) 1–19.
- 608 [10] B. Möller, M. Beer, *Fuzzy randomness: uncertainty in civil engineering and computational mechanics*, Springer Science & Business Media, 2004.
- 609 [11] S.-K. Au, J. L. Beck, Estimation of small failure probabilities in high dimensions by subset simulation, *Probabilistic Engineering Mechanics* 16 (4) (2001) 263–277.
- 610 [12] M. D. Shields, J. Zhang, The generalization of latin hypercube sampling, *Reliability Engineering & System Safety* 148 (2016) 96–108.
- 611 [13] S. Geyer, I. Papaioannou, D. Straub, Cross entropy-based importance sampling using gaussian densities revisited, *Structural Safety* 76 (2019) 15–27.
- 612 [14] B. Keshtegar, Z. Meng, A hybrid relaxed first-order reliability method for efficient structural reliability analysis, *Structural Safety* 66 (2017) 84–93.
- 613 [15] X. Huang, Y. Li, Y. Zhang, X. Zhang, A new direct second-order reliability analysis method, *Applied Mathematical Modelling* 55 (2018) 68–80.
- 614 [16] B. Echard, N. Gayton, M. Lemaire, Ak-mcs: an active learning reliability method combining kriging and monte carlo simulation, *Structural Safety* 33 (2) (2011) 145–154.
- 615 [17] G. Blatman, B. Sudret, Adaptive sparse polynomial chaos expansion based on least angle regression, *Journal of Computational Physics* 230 (6) (2011) 2345–2367.
- 616 [18] R. Teixeira, M. Nogal, A. O’Connor, Adaptive approaches in metamodel-based reliability analysis: A review, *Structural Safety* 89 (2021) 102019.
- 617 [19] Y.-G. Zhao, T. Ono, New point estimates for probability moments, *Journal of Engineering Mechanics* 126 (4) (2000) 433–436.
- 618
- 619
- 620
- 621
- 622
- 623
- 624
- 625
- 626
- 627
- 628
- 629
- 630
- 631
- 632
- 633
- 634
- 635

- 636 [20] S. Xiao, Z. Lu, Reliability analysis by combining higher-order unscented transformation and fourth-moment method,  
637 ASCE-ASME Journal of Risk and Uncertainty in Engineering Systems, Part A: Civil Engineering 4 (1) (2018) 04017034.
- 638 [21] J. Xu, C. Dang, A new bivariate dimension reduction method for efficient structural reliability analysis, Mechanical  
639 Systems and Signal Processing 115 (2019) 281–300.
- 640 [22] R. Liu, W. Fan, Y. Wang, A. H.-S. Ang, Z. Li, Adaptive estimation for statistical moments of response based on the exact  
641 dimension reduction method in terms of vector, Mechanical Systems and Signal Processing 126 (2019) 609–625.
- 642 [23] P. Wei, X. Zhang, M. Beer, Adaptive experiment design for probabilistic integration, Computer Methods in Applied  
643 Mechanics and Engineering 365 (2020) 113035.
- 644 [24] J. Li, J. Chen, Probability density evolution method for dynamic response analysis of structures with uncertain parameters,  
645 Computational Mechanics 34 (5) (2004) 400–409.
- 646 [25] G. Chen, D. Yang, A unified analysis framework of static and dynamic structural reliabilities based on direct probability  
647 integral method, Mechanical Systems and Signal Processing 158 (2021) 107783.
- 648 [26] D. Moens, M. Hanss, Non-probabilistic finite element analysis for parametric uncertainty treatment in applied mechanics:  
649 Recent advances, Finite Elements in Analysis and Design 47 (1) (2011) 4–16.
- 650 [27] B. Möller, W. Graf, M. Beer, Fuzzy structural analysis using  $\alpha$ -level optimization, Computational Mechanics 26 (6) (2000)  
651 547–565.
- 652 [28] C. Dang, P. Wei, M. G. Faes, M. A. Valdebenito, M. Beer, Interval uncertainty propagation by a parallel bayesian global  
653 optimization method, Applied Mathematical Modelling 108 (2022) 220–235.
- 654 [29] Z. Qiu, I. Elishakoff, Antioptimization of structures with large uncertain-but-non-random parameters via interval analysis,  
655 Computer Methods in Applied Mechanics and Engineering 152 (3-4) (1998) 361–372.
- 656 [30] S. Chen, H. Lian, X. Yang, Interval static displacement analysis for structures with interval parameters, International  
657 Journal for Numerical Methods in Engineering 53 (2) (2002) 393–407.
- 658 [31] R. R. Callens, M. G. Faess, D. Moens, Multilevel quasi-monte carlo for interval analysis, International Journal for Uncer-  
659 tainty Quantification 12 (4) (2022).
- 660 [32] B. Ni, C. Jiang, P. Wu, Z. Wang, W. Tian, A sequential simulation strategy for response bounds analysis of structures  
661 with interval uncertainties, Computers & Structures 266 (2022) 106785.
- 662 [33] M. C. Bruns, Propagation of imprecise probabilities through black box models, Ph.D. thesis, Georgia Institute of Tech-  
663 nology (2006).
- 664 [34] H. Zhang, R. L. Mullen, R. L. Muhanna, Interval monte carlo methods for structural reliability, Structural Safety 32 (3)  
665 (2010) 183–190.
- 666 [35] S. Au, Reliability-based design sensitivity by efficient simulation, Computers & Structures 83 (14) (2005) 1048–1061.
- 667 [36] P. Wei, J. Song, S. Bi, M. Broggi, M. Beer, Z. Lu, Z. Yue, Non-intrusive stochastic analysis with parameterized imprecise  
668 probability models: I. performance estimation, Mechanical Systems and Signal Processing 124 (2019) 349–368.
- 669 [37] P. Wei, J. Song, S. Bi, M. Broggi, M. Beer, Z. Lu, Z. Yue, Non-intrusive stochastic analysis with parameterized imprecise  
670 probability models: II. reliability and rare events analysis, Mechanical Systems and Signal Processing 126 (2019) 227–247.
- 671 [38] M. G. Faes, M. A. Valdebenito, D. Moens, M. Beer, Bounding the first excursion probability of linear structures subjected  
672 to imprecise stochastic loading, Computers & Structures 239 (2020) 106320.
- 673 [39] C. Dang, P. Wei, J. Song, M. Beer, Estimation of failure probability function under imprecise probabilities by active  
674 learning–augmented probabilistic integration, ASCE-ASME Journal of Risk and Uncertainty in Engineering Systems,  
675 Part A: Civil Engineering 7 (4) (2021) 04021054.
- 676 [40] P. Wei, F. Liu, M. Valdebenito, M. Beer, Bayesian probabilistic propagation of imprecise probabilities with large epistemic  
677 uncertainty, Mechanical Systems and Signal Processing 149 (2021) 107219.
- 678 [41] P. Wei, F. Hong, K.-K. Phoon, M. Beer, Bounds optimization of model response moments: a twin-engine bayesian active



- 679 learning method, *Computational Mechanics* 67 (5) (2021) 1273–1292.
- 680 [42] M. G. Faes, M. Daub, S. Marelli, E. Patelli, M. Beer, Engineering analysis with probability boxes: A review on computa-  
681 tional methods, *Structural Safety* 93 (2021) 102092.
- 682 [43] X. Yang, Y. Liu, Y. Gao, Y. Zhang, Z. Gao, An active learning kriging model for hybrid reliability analysis with both  
683 random and interval variables, *Structural and Multidisciplinary Optimization* 51 (5) (2015) 1003–1016.
- 684 [44] X. Yang, Y. Liu, Y. Zhang, Z. Yue, Hybrid reliability analysis with both random and probability-box variables, *Acta*  
685 *Mechanica* 226 (5) (2015) 1341–1357.
- 686 [45] X. Yang, Y. Liu, Y. Zhang, Z. Yue, Probability and convex set hybrid reliability analysis based on active learning kriging  
687 model, *Applied Mathematical Modelling* 39 (14) (2015) 3954–3971.
- 688 [46] J. Zhang, M. Xiao, L. Gao, J. Fu, A novel projection outline based active learning method and its combination with kriging  
689 metamodel for hybrid reliability analysis with random and interval variables, *Computer Methods in Applied Mechanics*  
690 *and Engineering* 341 (2018) 32–52.
- 691 [47] X. Chen, Z. Qiu, A novel uncertainty analysis method for composite structures with mixed uncertainties including random  
692 and interval variables, *Composite Structures* 184 (2018) 400–410.
- 693 [48] M. Xiao, J. Zhang, L. Gao, S. Lee, A. T. Eshghi, An efficient kriging-based subset simulation method for hybrid reliability  
694 analysis under random and interval variables with small failure probability, *Structural and Multidisciplinary Optimization*  
695 59 (6) (2019) 2077–2092.
- 696 [49] J. Song, P. Wei, M. Valdebenito, S. Bi, M. Broggi, M. Beer, Z. Lei, Generalization of non-intrusive imprecise stochastic  
697 simulation for mixed uncertain variables, *Mechanical Systems and Signal Processing* 134 (2019) 106316.
- 698 [50] X. Yuan, M. G. Faes, S. Liu, M. A. Valdebenito, M. Beer, Efficient imprecise reliability analysis using the augmented  
699 space integral, *Reliability Engineering & System Safety* 210 (2021) 107477.
- 700 [51] M. G. Faes, M. A. Valdebenito, X. Yuan, P. Wei, M. Beer, Augmented reliability analysis for estimating imprecise first  
701 excursion probabilities in stochastic linear dynamics, *Advances in Engineering Software* 155 (2021) 102993.
- 702 [52] C. Jiang, G. Lu, X. Han, L. Liu, A new reliability analysis method for uncertain structures with random and interval  
703 variables, *International Journal of Mechanics and Materials in Design* 8 (2) (2012) 169–182.
- 704 [53] M. G. Faes, M. A. Valdebenito, D. Moens, M. Beer, Operator norm theory as an efficient tool to propagate hybrid  
705 uncertainties and calculate imprecise probabilities, *Mechanical Systems and Signal Processing* 152 (2021) 107482.
- 706 [54] C. Jiang, J. Zheng, X. Han, Probability-interval hybrid uncertainty analysis for structures with both aleatory and epistemic  
707 uncertainties: a review, *Structural and Multidisciplinary Optimization* 57 (6) (2018) 2485–2502.
- 708 [55] J. Cockayne, C. J. Oates, T. J. Sullivan, M. Girolami, Bayesian probabilistic numerical methods, *SIAM Review* 61 (4)  
709 (2019) 756–789.
- 710 [56] D. R. Jones, M. Schonlau, W. J. Welch, Efficient global optimization of expensive black-box functions, *Journal of Global*  
711 *Optimization* 13 (4) (1998) 455–492.
- 712 [57] C. E. Rasmussen, C. K. I. Williams, *Gaussian Processes for Machine Learning*, MIT Press, 2006.
- 713 [58] C. E. Rasmussen, Z. Ghahramani, Bayesian monte carlo, *Advances in Neural Information Processing Systems* (2003)  
714 505–512.
- 715 [59] G. Li, S.-W. Wang, H. Rabitz, High dimensional model representations (HDMR): Concepts and applications, in: *Pro-*  
716 *ceedings of the Institute of Mathematics and Its Applications Workshop on Atmospheric Modeling*, Citeseer, 2000, pp.  
717 15–19.
- 718 [60] D. Huang, T. T. Allen, W. I. Notz, N. Zeng, Global optimization of stochastic black-box systems via sequential kriging  
719 meta-models, *Journal of Global Optimization* 34 (3) (2006) 441–466.
- 720 [61] N. Gayton, J. M. Bourinet, M. Lemaire, CQ2RS: a new statistical approach to the response surface method for reliability  
721 analysis, *Structural Safety* 25 (1) (2003) 99–121.

- 722 [62] R. Schöbi, B. Sudret, Structural reliability analysis for p-boxes using multi-level meta-models, *Probabilistic Engineering*  
723 *Mechanics* 48 (2017) 27–38.
- 724 [63] D. R. Karanki, H. S. Kushwaha, A. K. Verma, S. Ajit, Uncertainty analysis based on probability bounds (p-box) approach  
725 in probabilistic safety assessment, *Risk Analysis: An International Journal* 29 (5) (2009) 662–675.